JOC The Journal of Organic Chemistry

pubs.acs.org/joc Article

Structure–Property Relationship Study of *N*-(Hydroxy)Peptides for the Design of Self-Assembled Parallel β-Sheets

Alexis D. Richaud and Stéphane P. Roche*

Cite This: *J. Org. Chem.* 2020, 85, 12329–12342 Read Online

ACCESS | Metrics & More | Article Recommendations | Supporting Information

ABSTRACT: The design of novel and functional biomimetic foldamers remains a major challenge in creating mimics of native protein structures. Herein, we report the stabilization of a remarkably short β-sheet by incorporating *N*-(hydroxy)glycine (Hyg) residues into the backbone of peptides. These peptide–peptoid hybrids form unique parallel β-sheet structures by self-assembly upon hydrogenation. Our spectroscopic and crystallographic data suggest that the local conformational perturbations induced by *N*-(hydroxy)amides are outweighed by a network of strong interstrand hydrogen bonds.

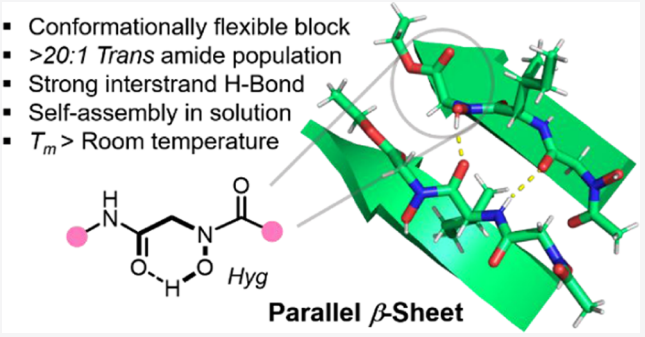

INTRODUCTION

In recent years, much interest has been devoted to the development of peptoids (*N*-substituted glycines)[1] due to their proteolytic stability and the ease to introduce various side chains without incorporating the asymmetric α-stereocenters typically found in peptides.[2] A major drawback in controlling these peptoid secondary structures is the lack of hydrogen-bonding motifs and the high backbone flexibility of the central glycine methylene. Interestingly, one subclass of peptoid blocks, namely, *N*-hydroxy-α-amino acids, can be found in numerous bioactive natural products, such as aurantimycins, polyoxypeptins, dentigerumycin, and penicisulfuranols A–F,[3] and other bacterial siderophores.[4] Despite an intriguing potential arising from the secondary hydroxamate functional group as a hydrogen-bond donor and acceptor, as well as a metal chelator,[5,6] the notorious lack of stability of this motif (pH-dependent decarboxylation and possible dismutation) has hampered most synthetic studies.[7] Seemingly, only sparse examples of synthetic and structural studies have been reported on the propensity of *N*-(hydroxy)glycine (Hyg) to induce secondary interactions like β-turn[8] and sheet-like structures (e.g., **1**, Figure 1).[9] Blackwell's study demonstrated that Hyg residues positioned at hydrogen-bonded (inward) sites in peptoid sequences like **1** enabled the formation of antiparallel β-sheets. Therefore, we hypothesized that by intercalating α-amino acids in such peptoids, sturdy *N*-(hydroxy)peptoid–peptide β-sheet hybrids (e.g., **2**, Figure 1) could potentially be generated. Given the important acidity of *N*-(hydroxyl)amides in comparison to typical amide groups,[10] we became interested in evaluating their hydrogen-bond donor/acceptor abilities to form β-sheets. *N*-(hydroxy)[9] and *N*-(alkoxy)peptoids[11] are known to preferentially adopt a trans-conformation, which is

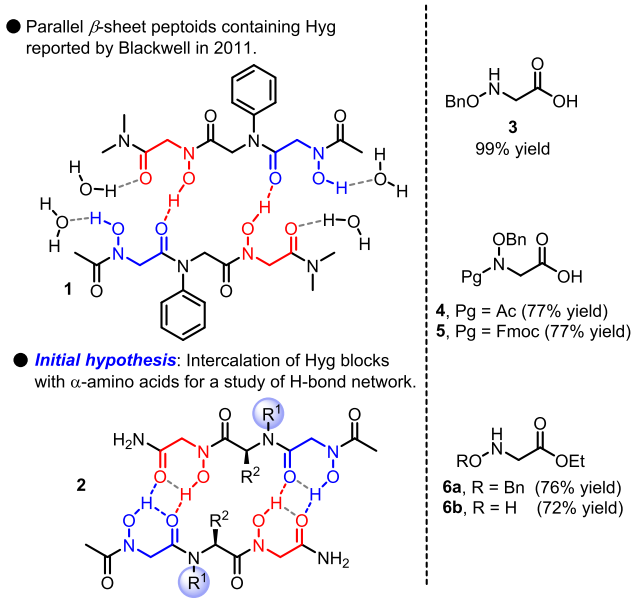

Figure 1. Proposed novel β-sheet scaffold built by intercalation of the Hyg blocks (left). Peptoid blocks synthesized in this study (right).

Received: July 1, 2020
Published: September 3, 2020

https://dx.doi.org/10.1021/acs.joc.0c01441
J. Org. Chem. 2020, 85, 12329–12342

also appropriate to the design of novel β-sheet tertiary structures. Herein, we report the stabilizing effect of Hyg blocks inside a unique intra/intermolecular hydrogen-bond network for the self-assembly of particularly short β-sheets (Figure 1).[12] This work provides a foundation to understand and rationalize the role of *N*-(hydroxy)amides as hydrogen-bond donor/acceptor motifs in the backbone of peptide−peptoid hybrids.

RESULTS AND DISCUSSION

Synthesis of Peptide−Peptoid Hybrids. The syntheses of *N*-hydroxy-α-amino acids in both racemic[13] and asymmetric[14] manners have been previously reported; however, the insertion of these peptoid blocks into peptides has been fairly scarce.[15] To develop a robust synthesis of *N*-(hydroxy)-peptoid−peptide hybrids, a series of *N*-(benzyloxy)glycine derivatives **3**−**6** were prepared with typical protecting groups for liquid- or solid-phase peptide synthesis (Figure 1). For the initial study of N-terminal elongation, dipeptide−peptoids **7a**−**c** were synthesized starting from *N*-(OBn)-Gly-OEt **6a**, which was coupled with three different Fmoc-protected amino acids (Scheme 1). As for *N*-alkyl peptoid blocks, *N*-alkoxy residues

Scheme 1. N-Terminal Elongation toward Tripeptide−Peptoids 9a−c

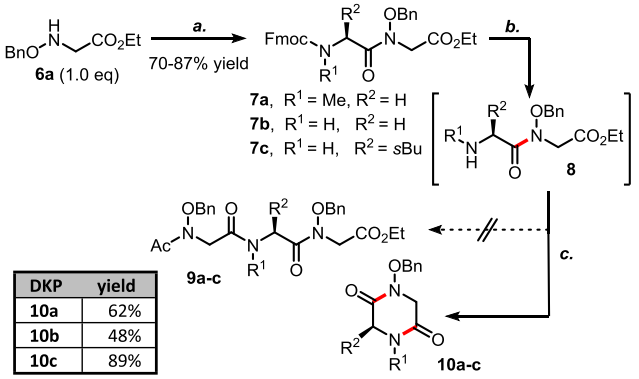

DKP	yield
10a	62%
10b	48%
10c	89%

[a]Reaction conditions: (a) Fmoc-AA-OH (4.0 equiv), HATU (4.0 equiv), HOAt (4.4 equiv), *N*,*N*-diisopropylethylamine (DIEA; 4.0 equiv) in CH_2Cl_2/DMF (3:1); (b) piperidine or $NHEt_2$; (c) **3** (4.0 equiv), HATU (4.0 equiv), HOAt (4.4 equiv), DIEA (4.0 equiv) in CH_2Cl_2.

are known to have a low reactivity for amide-bond formation, but a cocktail of HATU/HOAt reagents was found suitable to the synthesis of dipeptide−peptoids **7a**−**c** in 70−87% yields. Compounds **7a**−**c** were then engaged in a sequence of deprotection/coupling toward the tripeptide−peptoids **9a**−**c**. Unfortunately, under the large set of conditions tested,[16] N-terminal free dipeptide **8** proved difficult to isolate and the coupling toward **9a**−**c** failed. Instead, large amounts of degradation were observed along with the intramolecular cyclization into diketopiperazines (DKPs) **10a**−**c**. Although Hyg favors trans amide bonds thermodynamically, the low transition-state energy barrier previously reported for the cis−trans isomerization of this motif (~16 kcal/mol)[7b] can explain the ease of forming DKPs. While *N*-(benzyloxy)peptoid oligomers are known to be exclusively in a most stable trans amide conformation,[11] the fast kinetics of cis−trans isomerization do not allow the cis rotamer to be observed on the NMR time scale. To obtain a direct evidence of the genuine cis−trans isomerization, we thought to force the equilibrium toward the cis rotamer by exploiting the chelating nature of the Hyg residue. Dipeptide−peptoid **7c** was therefore hydrogenated to the corresponding Fmoc-Ile-Hyg-OEt dipeptide, which was used as the chelating ligand to form a gallium(III) complex (3:1 ligand/metal ratio).[17] In this complex, the strong nuclear Overhauser effect spectroscopy (NOESY) $^1H-^1H$ cross-peak signal between the Ile H_α and the Hyg methylene detected by NMR supports the presence of a *cis* *N*-(hydroxy)amide rotamer. Taken together, this spectroscopic evidence of a cis rotamer and the facile DKP formation (**8** → **10**) further support that *N*-(hydroxy) and *N*-(benzyloxy)-amides undergo fast cis−trans isomerization.

To circumvent the formation of DKP **10**, we turned our attention to a strategy of C-terminal elongation (Scheme 2).

Scheme 2. C-terminal Elongation toward Tripeptide−Peptoids 12a−d

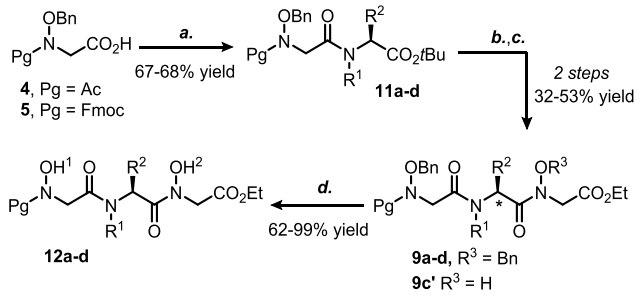

[a]Reaction conditions: (a) from **4** (1.0 equiv), DIPEA (1.5 equiv), for **11a,b**: EDCi (1.2 equiv), HOBt (1.2 equiv) in CH_2Cl_2, for **11c**: H-AA-O*t*Bu (2.0 equiv), HATU (1.5 equiv), HOAt (1.5 equiv) in dimethylformamide (DMF); for **11d**: from **5** (1.0 equiv), EEDQ (1.2 equiv) in CH_2Cl_2; (b) TFA/CH_2Cl_2 (1:1); (c) for **9a**−**c**′: **6a** or **6b** (2.0 equiv), HATU (2.0 equiv), HOAt (2.0 equiv), DIEA (2.0 equiv) in DMF, for **9d**: PivCl (1.2 equiv), lutidine (1.2 equiv) in CH_2Cl_2; (d) Pd/C 10 mol %, H_2 in EtOH.

Dipeptides **11a**−**c** were synthesized by coupling the acetyl Hyg **4** with three different *t*-butyl α-amino esters by activation with EDCi or HATU. When similar conditions were tested to couple Fmoc-Hyg **5** with Ile-O*t*Bu, an unexpected cleavage of the benzyl protecting group occurred. The coupling was therefore optimized with *N*-ethoxycarbonyl-2-ethoxy-1,2-dihydroquinoline (EEDQ) to deliver dipeptide **11d** without epimerization.[18] A smooth deprotection with trifluoroacetic acid (TFA) leads quantitatively to all of the corresponding free carboxylic acid of dipeptides **11a**−**d**, which were directly coupled with **6a** in the presence of HATU/HOAt to deliver tripeptide−peptoids **9a**−**d**. Unfortunately, **9c** was highly epimerized at the Ile α-stereocenter (2:3 dr). To improve the pivotal amide-bond formation, the coupling reaction was further evaluated with the unprotected block **6b**. In this case, the epimerization of tripeptide−peptoids **9c**′ could not be detected by ^1H NMR, but the racemization was later confirmed by the presence of a mixture of Ile/allo-Ile residues in the crystal structure of **12c** (Figure 2). *N*-(hydroxy) and *N*-(benzyloxy)glycine blocks are less reactive than typical *N*-methylated amino acids, which are already known to be poor nucleophiles in amide-bond formation. Due to the oxygen electronegativity and the steric hindrance carried by the

https://dx.doi.org/10.1021/acs.joc.0c01441
J. Org. Chem. 2020, 85, 12329−12342

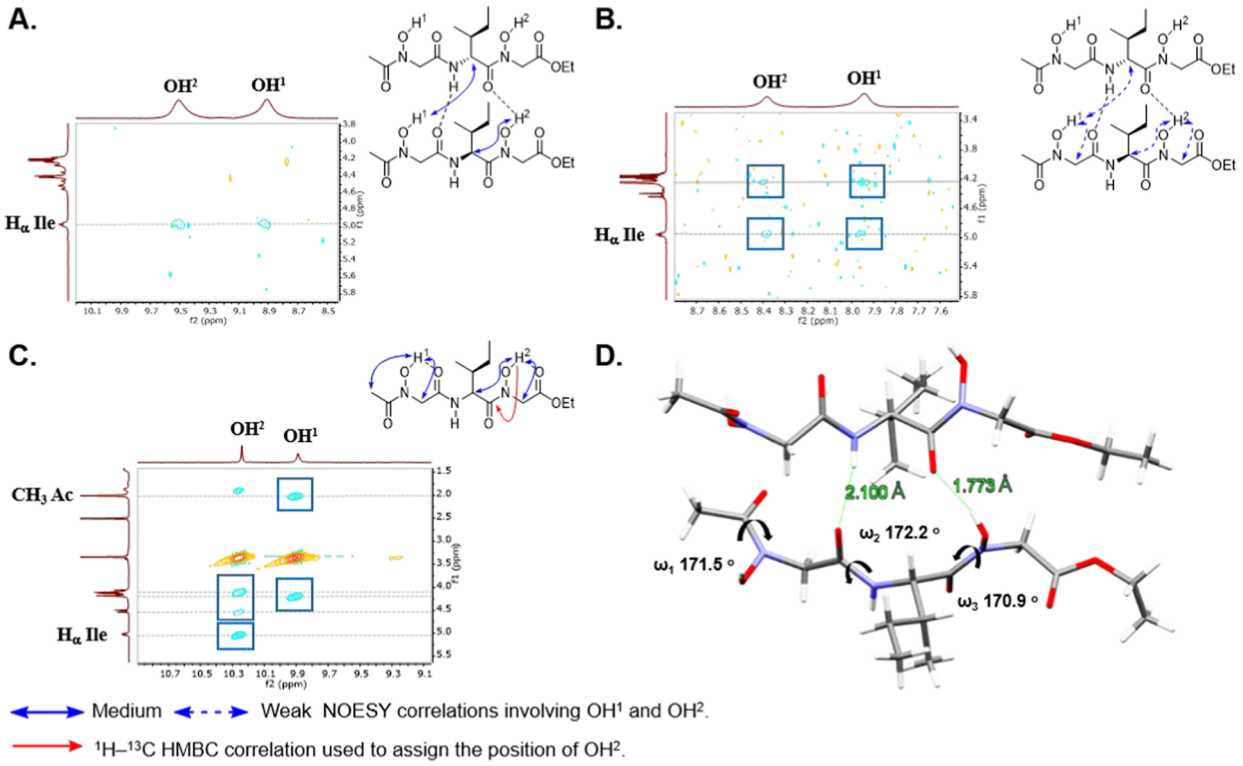

Figure 2. NOESY data of **12c** in the region of the N-OH protons (A) in $CDCl_3$, (B) in CD_3CN, and (C) in DMSO-d_6. (D) X-ray structure of **12c** showing the solid-state conformation with interstrand hydrogen bonds represented by the dashed lines in the parallel β-sheet.

hydroxy- and benzyloxy-side chains during the approach to the activated carbonyl π^* orbital, such peptoid ligation is particularly slow and difficult, leading ultimately to potential epimerization. To address this issue, several activating cocktails were evaluated for the difficult coupling of **6a**. To our delight, tripeptide−peptoid **9c** was prepared with ∼17% of epimerization using EEDQ as the activating agent. Given the electron-withdrawing nature of the *N*-(benzyloxy) side chain, we hypothesized that the N-terminal acetyl of **11c** might be unusually basic and participates into the Ile epimerization (see Figure SI-1). Thus, by switching to a Fmoc-protecting group in **11d**, the EEDQ coupling was achieved successfully to produce **9d** in 21% yield with minimal epimerization (∼3%).[16,18] To circumvent the low coupling yield, further optimizations were required. A cocktail of pivaloyl chloride with lutidine (hindered base) provided tripeptide−peptoid hybrid **9d** in 50% yield with low epimerization (<5%).[16] Finally, benzyl groups from all synthetic tripeptide−peptoids **9a−d**, **9c′** were removed under typical hydrogenation conditions to afford **12a−d** in 79−99% yields.

Structural Analysis of the Peptide−Peptoid Hybrids by Nuclear Magnetic Resonance (NMR) Spectroscopy. The synthesis of "turnless" β-sheets inspired by short protein sequences or by peptidomimetics remains a major challenge.[19] Indeed, motifs capable of enhancing nonbonded interstrand interactions to stabilize artificial short β-sheets are rare.[20] To assess the presence of secondary and potential tertiary structures in the synthetic peptide−peptoid hybrids **9a−d**, **9c′**, and **12a−d**, a careful solution NMR spectral analysis at 18 °C was performed (Figure 2A−C).[16,21] A combination of ^{1}H, ^{1}H−^{1}H NOESY, and ^{1}H−^{13}C heteronuclear multiple-quantum correlation (HMBC) NMRs in solvents of various polarity ($CDCl_3$, CD_3CN, DMSO-d_6) facilitated the conformational and structural analyses of these peptoid−peptide hybrids.[16] The cis−trans equilibrium constants for both *N*-(benzyloxy) and *N*-(hydroxy)glycine residues in peptides **7a**, **11a**, and **9a** were obtained with $K_{trans/cis}$ values > 20 in each case, meaning that independently of the solvent, these amides have an exclusive thermodynamic preference for the trans geometry.[16,22] Interestingly, in all constructs **9**, **11−12**, the methylene protons ($H_\alpha/H_{\alpha'}$) of *N*-(hydroxy) or *N*-(benzyloxy)glycine blocks are always highly diastereotopic (doublets with a geminal coupling constant of ∼17 Hz) with a $\Delta\delta(H_\alpha/H_{\alpha'})$ of ∼0.5 ppm, which typically characterize well-folded structures. Each hydroxyl proton OH^1 and OH^2 from Hyg(1) and Hyg(2) residues was easily assigned and differentiated based on distinct NOESY correlations as well as a clear HMBC correlation between OH^2 and the vicinal Ile carbonyl. Given the downfield chemical shifts of both OH^1 (δ 8.36−8.76 and 9.73−9.91 ppm) and OH^2 (δ 8.85−9.44 and 10.19−10.25 ppm) in $CDCl_3$ and DMSO-d_6, respectively, tripeptide−peptoids **9c′** and **12a−d**, hydroxyl hydrogens were determined to participate in inter- or intramolecular hydrogen bonds. A deshielding of ∼0.5 ppm between δ OH^1 and OH^2 suggests that the OH^2 hydroxyl is more strongly hydrogen bonded and likely to participate in the β-sheet stabilization. As shown in Figure 2C, all NOESY cross-peaks obtained for **12c** in DMSO-d_6 can be attributed to interstrand interactions suggesting that no intermolecular assembly occurs in this solvent. In contrast, in CD_3CN and more markedly in $CDCl_3$ (Figure 2A,B), a stronger NOESY correlation between OH^1 on one strand and the Ile H_α on the second strand supports the formation of a β-sheet self-assembly. Indeed, in a pair of facing residues *i*,*j* on the opposite strands from a parallel β-sheet (e.g., Ile/allo-Ile in **12c,d**) residue *i* is H-bonded to both residues $j-1$ and $j+1$, which in this case both are Hyg residues.[23] As established by

https://dx.doi.org/10.1021/acs.joc.0c01441
J. Org. Chem. 2020, 85, 12329−12342

Abraham, the difference in chemical shits of exchangeable protons or chemical shift deviation (CSD) due to solvent exposure $\Delta\delta = \delta(\text{DMSO-}d_6) - \delta(\text{CDCl}_3)$ can be used to assess the strength of intra- and intermolecular hydrogen bonds for the OH and NH groups.[24] The $\Delta\delta(H_N)$ of 0.53 and 0.57 ppm in constructs **12c,d** suggest the presence of relatively strong hydrogen bonds likely arising from an intermolecular interaction between β-strands (see Table SI-8). Similarly, $\Delta\delta(OH^2)$ of 0.80 and 0.77 ppm in **12c** and **12d**, respectively, support the existence of hydrogen bonds from the Hyg(2) hydroxyls, while the larger $\Delta\delta(OH^1)$ of 1.13 and 1.11 ppm firmly indicate that OH^1 hydroxyls are more solvent-exposed and not engaged in hydrogen bonding.[16] Collectively, the downfield shifts observed for the exchangeable protons (OH/H_N) as well as the small CSD values for both Ile H_N and Hyg(2) OH in constructs **12c,d** suggest that such hydrogens participate in strong interstrand hydrogen bonding. Furthermore, the self-assembly of **12c** was characterized by monitoring the chemical shift deviations of OH/H_N protons as a function of concentration in $CDCl_3$ (Figures SI-12 and SI-13).[16,21] In the range of concentrations studied, changes in chemical shifts values fitted well to a dimerization isotherm equation representing the assembly of the strands into β-sheets.[20a] These results also suggest that upon hydrogenation of the *N*-(benzyloxy)glycine residues, Hyg blocks play an important role in the self-assembly of constructs **12a−d** into short β-sheets.

X-ray Analysis. The structural features of β-sheets revealed by the NMR study were further confirmed in the crystal structure of construct **12c** obtained by X-ray analysis (Figure 2D). In this crystal, the parallel β-sheets are packed in a head-to-head manner forming columns through a single and relatively weak hydrogen bond $OH^1\cdots O$ = C (N-terminal acetyl). Certainly, the low-lying conformation observed in the crystal lattice reflects closely the major conformer of **12c** in solution ($CDCl_3$). Both H_N and OH^2 groups are shown to participate in intermolecular hydrogen bonding to stabilize a parallel β-sheet structure. Both Φ and ψ dihedral angles of Hyg(1/2) and Ile residues collected from the crystal structure are in agreement with an extended β-sheet arrangement (see the Ramachandran plot, Figure SI-14). A notable feature of the parallel β-sheet is the nitrogen pyramidalization in each *N*-(hydroxy)amide ($\omega(OH^1)$ 171.5° and $\omega(OH^2)$ 170.9°). A similar pyramidalization was previously reported by Kirshenbaum[11] and others[25] for *N*-alkoxy peptoids. This phenomenon is likely responsible for decreasing the nitrogen lone pair resonance in the *N*-(hydroxy)amide, which in turn accentuates the basicity of the vicinal carbonyl. This stereoelectronic effect likely explains the unique hydrogen-bond acceptor nature of the *N*-(hydroxy)amide carbonyl responsible for the unusual parallel β-sheet alignment. In the original report from Blackwell, the central α-amino acid was instead a *N*-aryl peptoid block (i.e., construct **1** vs **2**, Figure 1). In such constructs, the central carbonyls were also good hydrogen-bond acceptors, but these peptoid blocks could not participate in intermolecular H-bond, which could justify the preference for an antiparallel β-sheet direction. Our results on peptoid−peptide hybrids **12a−d** complement well Blackwell's study on peptoids in which Hyg residues were positioned at the H-bonded inward sites of the antiparallel β-sheets.[9] Herein, we demonstrated that *N*-(hydroxy)amide groups can force intermolecular hydrogen bonds with Hyg at both H-bonded and non-H-bonded sites (inward and outward of strands) for stabilizing these novel β-sheets with a different parallel directionality.[26]

β-Sheet Self-assembly and Thermal Stability. Secondary and tertiary peptidyl structures have well-established signatures in far-UV circular dichroism (CD), but the assignment of the bands in the peptoids is more challenging due to their important flexibility. *N*-Alkoxy peptoid oligomers have been proposed by Kirshenbaum to adopt a polyproline II type (PPII) secondary structure that exhibit two maxima at 197 and 215 ± 5 nm.[27] The CD spectra obtained for tripeptide−peptoid hybrid **9d** present similar bands at 195/216 nm in CH_3CN and 200/218 nm in HFIP, suggesting that a similar PPII secondary structure formed (Figure 3). As

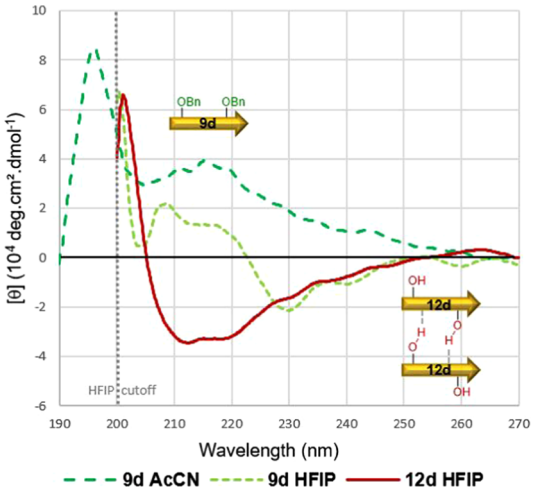

Figure 3. CD spectra comparison of **9d** and **12d** showing the self-assembly process a CD spectra of **9d** in acetonitrile (90 mM) and HFIP (103 mM) and of **12d** in HFIP (116 mM) at 0 °C. Sample concentrations were accurately determined by UV-absorption of the fluorene (Fmoc) chromophore.

shown by the superimposition of the CD spectra in Figure 3, the hydrogenation of **9d** into **12d** triggers a dramatic change in the tripeptide−peptoid 3-dimensional structure. Typically, antiparallel β-sheets are characterized by two bands, a positive maximum at 193−195 nm and a negative exciton at 213−218 nm, profoundly resembling the two bands for parallel β-sheets at 200−203 and 214−221 nm.[28] Therefore, the combination of a positive exciton at 201 nm and a large CD band overlay at 213−219 nm obtained for construct **12d** conclusively supports the formation of a parallel β-sheet. Furthermore, a positive band at 298 nm, characteristic of a $\pi-\pi^*$ transition, was also observed in the near-UV CD spectrum of **12d** (Figure SI-15C).[29] This band arising from an interaction between the proximate fluorenyl π-systems of N-terminal Fmoc groups also supports the existence of a parallel arrangement between β-strands. Overall, the structural elucidation by CD from the Fmoc interaction at 298 nm and the exciton minima at 213/219 nm distinctively confirm a parallel β-sheet self-assembly of **12d** in solution.

To test the stability of these novel parallel β-sheets, variable temperature NMR spectra (VT-NMR) were recorded between −60 and 110 °C (Figure 4). As expected, the spectra of tripeptide−peptoids **12c,d** in DMSO-d_6 revealed no evidence of tertiary structures as shown by the small-temperature dependence coefficients (T_C, $\Delta\delta/T$ < −4.6 ppb/K) for H_N, while both *N*-(hydroxy)amide hydrogens (OH^1/OH^2) might

https://dx.doi.org/10.1021/acs.joc.0c01441
J. Org. Chem. 2020, 85, 12329−12342

A.

Constructs	T_C $CDCl_3$ Δδ/ΔT (ppb/K)			T_C DMSO-d_6 Δδ/ΔT (ppb/K)		
	NH	OH^1	OH^2	NH	OH^1	OH^2
9c'	-4.2	N/A	-13.6	-5.9	N/A	-4.6
***trans*-12a**	N/A	-14.2	-17.0	N/A	-6.1	-4.2
***cis*-12a**	N/A	-5.8	-15.8	N/A	-5.5	-4.5
12b		*Not soluble*		-5.3	-4.5	-4.2
12c	-8.2	-12.2	-12.7	-5.6	-4.0	-4.6
12d	-8.7	-15.6	-12.6	-5.5	-3.7	-4.7

B.

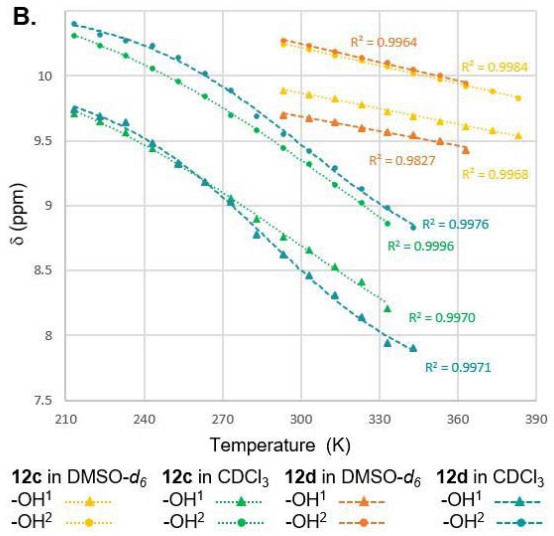

Figure 4. (A) Temperature dependence of the H_N and OH chemical shifts. (B) Plots of hydroxyl proton (OH^1/OH^2) chemical shifts as a function of temperature in DMSO-d_6 and $CDCl_3$.

exist in a relatively strong intramolecular hydrogen bond (−4.6 < T_C < −4.0 ppb/K).[30,31] The T_C representing the slopes of the best-fitted linear regression of OH^1 and OH^2 chemical shift drifts as a function of temperature were invariably low for all of the constructs studied in DMSO-d_6 (Figure 4A and Table SI-7). It can be concluded that a strong intramolecular six-membered ring hydrogen bond stabilizes each Hyg residue in DMSO-d_6 in single-stranded molecules (Figures SI-6 and SI-7).[16] In contrast, the significantly larger $T_C(OH^1)$ and $T_C(OH^2)$ values (−17.0 < T_C < −12.2 ppb/K) in $CDCl_3$ (Figure 4A) indicate that the hydrogen bonds are weaker in apolar solvents. These counterintuitive results could be explained by the competition between a strong interstrand H-bond and the innate intramolecular H-bond of the Hyg residues (as shown in DMSO-d_6). Competing intra- and intermolecular H-bonds result in a net weakening of the hydroxyls' hydrogen-bond network. The results obtained for β-sheets **12c,d** are in line with the interactions reported earlier by Blackwell for a peptoid tetramer β-sheet (e.g., **1**, Figure 1). While examining the temperature dependency on the *N*-(hydroxy)amide chemical shifts in $CDCl_3$, it was found that both hydroxyl signals shifted in a nonlinear fashion (Figure 4B). The sigmoidal dependence of *N*-(hydroxy)amide proton (OH^1/OH^2) chemical shifts as a function of temperature is distinctive of a β-sheet denaturation transition.[32] The melting curves observed for β-sheets **12c,d** indicate a rupture of folding at elevated temperatures. Thus, melting temperatures (T_m) corresponding to the hydrogen-bond network cleavage within the parallel β-sheets of **12c,d** were estimated from the best-fitted curves of thermal transition to the Boltzmann equation.[16] $T_m(OH^1)$ of 23 and 14 ± 5 °C and $T_m(OH^2)$ of 46 and 29 ± 5 °C were calculated for the β-sheets of **12c** and **12d**, respectively (Figure 4B, Table SI-6). In both molecules, the significantly higher melting temperature (>15 °C) associated with the H-bond rupture of hydroxyl OH^2 is a direct evidence that the interstrand hydrogen bond from Hyg(2) stabilizes the entire structure.

CONCLUSIONS

In conclusion, a coupling of the readily available *N*-(hydroxy)-glycine peptoid blocks (Hyg) has been developed with a low epimerization rate (3−5%) for C- and N-terminal insertion into peptide−peptoid hybrids. The synthetic constructs self-assembled in solution to form short parallel β-sheets, which were characterized by a combination of NMR and CD experiments and confirmed by the crystal structure of **12c**. A detailed examination of the major differences in NOESY cross-strand correlations, CSDs, T_C, and T_m in various solvents clearly highlights the role of *N*-(hydroxy)amides from Hyg residues in the self-assembly and the stabilization of these tertiary structures.[8a] Our results demonstrated that *N*-(hydroxy)amides not only favor exclusively trans amide conformers via intramolecular H-bonds ($K_{trans/cis}$ > 20) but are also amenable to strong interstrand hydrogen bonds in solvents of low polarity. Recent studies from Del Valle have shown that the insertion of *N*-(amino)[33] and *N*-(hydroxy) α-amino acids[15f] at specific non-hydrogen-bonded sites (outward positions) can stabilize the β-sheets within hairpins. In contrast, the present study establishes that a combination of *N*-(hydroxy)amides at hydrogen-bonded (inward) and non-hydrogen-bonded outward sites can be favorable due to a strong intramolecular and interstrand H-bond network. Given the typical difficulty to create stable β-sheets within short peptide constructs,[19,20] the ability of Hyg to improve the hydrogen-bond donor/acceptor properties of proteinogenic backbone amides will certainly find numerous applications in foldamer chemistry. Ongoing studies in our laboratory will leverage the unique stereoelectronic properties of Hyg and other *N*-hydroxy α-amino acids to study the assembly of the parallel and antiparallel β-hairpins in water.[34]

EXPERIMENTAL SECTION

General Information. All reagents used in the present paper were acquired from Alfa Aesar, Acros Organics, or Sigma Millipore. All bulk solvents were acquired from Fischer Scientific. Freshly distillated solvents were used in the reactions presented herein. Chloroform was dried over $CaCl_2$ overnight prior to distillation (BP 61 °C) and transferred under an argon atmosphere to a dark glass bottle with 3 Å molecular sieves for storage. Tetrahydrofuran was purified by refluxing with and distilling from sodium with benzophenone and transferred under an argon atmosphere to a dark glass bottle for storage. Dichloromethane was dried over $CaCl_2$ overnight prior to distillation (BP 40 °C) and transferred under an argon atmosphere to a dark glass bottle with 3 Å molecular sieves for storage. Toluene was dried over $CaCl_2$, CaH_2, or $CaSO_4$ and molecular sieves and transferred under an argon atmosphere to a dark glass bottle for storage. Full procedures can be found in Purification of Laboratory Chemicals by Armarego, W. L.F., and Chai C. L. L. editor (sixth edition). Reactions were performed in flame-dried glassware under a positive pressure of argon, unless the reaction occurs in water or aqueous solvent. Yields refer to chromatographically and spectroscopically pure compounds, unless otherwise noted. Analytical thin-layer chromatography (TLC) was performed on 0.25 mm glass-backed 60 Å F-254 TLC plates. Flash chromatography was performed using 230−400 mesh silica gels

https://dx.doi.org/10.1021/acs.joc.0c01441
J. Org. Chem. 2020, 85, 12329−12342

(Silicycle, Inc.). The plates were visualized by exposure to UV light (254 nm) and developed by a solution of phosphomolybdic acid in ethanol, vanillin/sulfuric acid in ethanol, ninhydrin in ethanol, potassium permanganate in water/potassium carbonate/sodium hydroxide, or cerium-ammonium-molybdate in water/sulfuric acid and heat. Melting points were determined using an MPA 160 digital melting point apparatus. The matrix-assisted laser desorption/ionization-time of flight (MALDI-TOF) mass spectra were performed on a Microflex LRF MALDI-TOF. The high-resolution mass spectra (HRMS) were obtained from the University of Florida using an Agilent 6230 TOF instrument, using electrospray ionization (ESI). The infrared spectra were recorded on a Nicolet iS10 FT-IR spectrophotometer (Thermo Scientific) with a SMART iTX ATR accessory. Optical rotation was measured on a JASCO P-2000 polarimeter.

The ^{1}H NMR spectra were recorded on a Varian Mercury400 (400 MHz) spectrometer using Vnmrj 4.2 software, Bruker AV-400 Ultrashield (400 MHz) spectrometer using Topspin 3.5 software, or Varian Mercury500 (500 MHz) spectrometer using Vnmrj 4.2 software and are reported in ppm using solvent as an internal standard (C_6D_6 at 7.16 ppm, $CDCl_3$ at 7.26 ppm, CD_3CN at 1.94 ppm, CD_3OD at 3.31 ppm, DMSO-d_6 at 2.50 ppm, and 1,4-dioxane-d_8 at 3.53 ppm). Data are reported as (br = broad, s = singlet, d = doublet, t = triplet, q = quartet, p = pentet, m = multiplet; coupling constant(s) in hertz, integration). The ^{13}C NMR spectra were recorded on a Bruker (100 MHz) spectrometer. Chemical shifts are reported in ppm, with solvent resonance employed as the internal standard (C_6D_6 at 128.1 ppm, $CDCl_3$ at 77.2 ppm, CD_3CN at 118.3 and 1.3 ppm, CD_3OD at 49.0 ppm, and DMSO-d_6 at 39.5 ppm). The NOESY spectra were recorded at 291 K, in the solvents mentioned above, at concentrations of 5−10 mM, with a 300 ms mixing time.

Variable temperature NMR were recorded on a Varian Mercury400 (400 MHz) spectrometer. The range of temperature studied was −60−70 °C in $CDCl_3$, −40−80 °C in CD_3CN, 0−100 °C in dioxane-d_8, and 20−110 °C in DMSO-d_6. The spectra were recorded with 16 scans every 10 °C, with a 5 min stabilization at each temperature before data acquisition. A final spectrum was recorded afterward at 20 °C to verify the absence of decomposition or transformation of the sample.

The CD spectra were recorded on a JASCO J-810 spectropolarimeter with a temperature controller module JASCO PFD-425S. The samples were prepared in a concentration range between 30 and 200 μM in CH_3CN or HFIP, and the sample concentrations were accurately determined by measuring the sample's absorbance using a JASCO V-670 spectrophotometer based off the UV-absorption of the fluorenyl (Fmoc) group (ε_{290} = 6089 M^{-1} cm^{-1}) at 290 nm. The concentrations were obtained based on the Beer law: $c = A/(\varepsilon \cdot l)$, with c the sample concentration, A the measured absorptivity, ε the molar absorptivity, and l the path length of the cuvette. The raw CD data were recorded in mdeg with eight scans from 185 to 270 nm for the far-UV and 270−350 nm for the near-UV, every 0.1 nm at a speed of 100 nm per min. The CD spectra of the blank (pure solvent) were recorded and subtracted, while the baseline was set to 0 mdeg between 260 and 270 nm for the far-UV and 330−340 nm for the near-UV. The spectra were smoothed and baseline-corrected using the Spectragryph 1.2 software,[35] then converted into molar elipticity (deg cm^2 $dmol^{-1}$). The products of functionalization **3**, **6a**, **6b**, **SI-1**, and **SI-2** have been reported previously and characterized in refs 36d,c,b,e,a, respectively.

*Synthesis of N-(benzyloxy)glycine (**3**).*

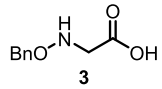

3

$C_9H_{11}NO_3$

MW 181.07 g.mol^{-1}

O-Benzyl hydroxylamine hydrochloride (5.00 g, 31.1 mmol, 1.0 equiv) and glyoxylic acid monohydrate (4.33 g, 47.0 mmol, 1.5 equiv) were solubilized in AcOH/water (1:1 v/v, 100 mL) and stirred at RT during 30 min (completion monitored by TLC, oxime intermediate, R_f = 0.8, EtOAc/MeOH 1:1 v/v). The mixture was cool down to 0 °C with an ice bath and a solution of sodium cyanoborohydride (7.90 g, 125 mmol, 4.0 equiv) in AcOH/water (1:1 v/v, 50 mL) was added portion wise to avoid byproduct formation. The mixture was stirred for 5 h at RT. The reaction completion was monitored by TLC until the disappearance of the oxime intermediate. Water was then added and the crude reaction mixture was extracted with a mixture of *i*PrOH/$CHCl_3$ (5 × 20 mL). The combined organic layers were washed with saturated brine (3 × 20 mL), dried over Na_2SO_4, and filtrated, and the solvent was removed under reduced pressure (T < 35 °C) to afford **3** as a white solid (5.60 g, 30.9 mmol, 99% yield). R_f = 0.6 (100% EtOAc); HRMS-ESI (m/z): $[M + H]^+$ calcd for $C_9H_{12}NO_3$, 182.0812; found, 182.0810 (−1.1 ppm). *N*-(Benzyloxy)-glycine **3** was pure enough to be engaged directly in the second step.

*N-Acetyl-N-(benzyloxy)glycine (**4**).*

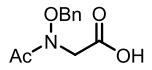

4

$C_{11}H_{13}NO_4$

MW 223.08 g.mol^{-1}

Compound **3** (3.00 g, 16.6 mmol, 1.0 equiv) and sodium carbonate (1.76 g, 16.6 mmol, 1.0 equiv) were solubilized in water (17 mL). Acetic anhydride (1.86 g, 18.2 mmol, 1.1 equiv) was then added dropwise resulting in a precipitation and a yellow coloration. The mixture was stirred for an additional 30 min at RT. An initial wash using diethyl ether (2 × 20 mL) was achieved directly from the crude reaction mixture, and then, the aqueous layer was acidified with a solution of 2.0 M HCl to pH ∼ 3. The aqueous layer was extracted with dichloromethane (3 × 20 mL), the combined organic layers were dried over Na_2SO_4, filtrated, and the solvent was evaporated under reduced pressure to afford product **4** in a pure form as a yellowish powder (2.86 g, 12.8 mmol, 77% yield). R_f = 0.7 (EtOAc/MeOH 7:3 v/v); mp 109.0−115.0 (±0.6) °C; IR ν_{max}: 2928, 1706, 1596, 1456, 1379, 1260, 964, 911, 847, 749 cm^{-1}; ^{1}H NMR (400 MHz, $CDCl_3$, δ): 9.97 (br, 1H), 7.37 (s, 5H), 4.87 (s, 2H), 4.31 (s, 2H), 2.15 (s, 3H); ^{13}C{^{1}H} NMR (100 MHz, $CDCl_3$, δ): 175.0, 172.5, 134.2, 129.5 (2C), 129.2, 128.8 (2C), 77.5, 49.4, 20.2; HRMS-ESI (m/z): $[M + Na]^+$ calcd for $C_{11}H_{13}NO_4Na$, 246.0737; found, 246.0728 (−3.7 ppm).

*N-(((9H-Fluoren-9-yl)methoxy)carbonyl)-N-(benzyloxy)glycine (**5**).*

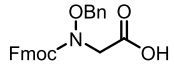

5

$C_{24}H_{21}NO_5$

MW 403.14 g.mol^{-1}

Compound **3** (1.00 g, 5.52 mmol, 1.0 equiv) and sodium bicarbonate (928 mg, 11.0 mmol, 2.0 equiv) were solubilized in water (10 mL) by stirring 10 min at RT. The mixture was cooled down to 0 °C and (9*H*-fluoren-9-yl)methyl chloroformate (1.71 g, 6.63 mmol, 1.2 equiv) in dioxane (10 mL) was added to the mixture and stirred for 2 h at 0 °C. The dioxane was evaporated under reduced pressure, a solution of saturated sodium bicarbonate was added (pH ∼ 9), and the aqueous phase was washed with hexanes (20 mL). The resulting aqueous layer was acidified with a solution of HCl (2.0 M) to pH ∼ 4 allowing for the product precipitation. The product was extracted with dichloromethane (3 × 20 mL), the combined organic layers were dried over Na_2SO_4, filtrated, and the solvent was evaporated under reduced pressure. The crude product was purified by precipitation into petroleum ether at RT and then filtrated to afford product **5** in a pure form as a white powder (1.73 g, 4.29 mmol, 77% yield). R_f = 0.7 (100% EtOAc); mp 132.0−137.0 (±0.6) °C; IR ν_{max}: 3039, 2954, 1757, 1737, 1666, 1427, 1350, 1248, 1184, 1116, 872, 760, 733 cm^{-1}; ^{1}H NMR (400 MHz, CD_3OD, δ): 7.77 (d, J = 7.5 Hz, 2H), 7.64 (d, J = 7.4 Hz, 2H), 7.37 (t, J = 7.3 Hz, 2H), 7.30 (m, 5H), 7.23 (m, 2H), 4.64 (s, 2H), 4.58 (d, J = 6.0 Hz, 2H), 4.25 (t, J = 6.0 Hz, 1H), 4.02 (s, 2H); ^{13}C{^{1}H} NMR (100 MHz, DMSO-d_6, δ): 169.9, 157.3, 144.1 (2C), 141.4 (2C), 135.5, 129.9 (2C), 128.9, 128.7 (2C), 128.2 (2C),

https://dx.doi.org/10.1021/acs.joc.0c01441
J. Org. Chem. 2020, 85, 12329−12342

127.6 (2C), 125.5 (2C), 120.6 (2C), 76.5, 67.3, 51.6, 47.1; HRMS-ESI (m/z): $[M + H]^+$ calcd for $C_{24}H_{22}NO_5$, 404.1492; found, 404.1485 (−1.7 ppm).

Substrates 6a and 6b were Prepared by the Following Procedures.

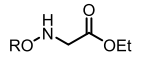

6a: R=Bn, $C_{11}H_{15}NO_3$
6b: R=H, $C_4H_9NO_3$

The appropriate alkoxyamine hydrochloride (1.0 mmol, 1.0 equiv), *p*-toluenesulfonic acid (0.1 mmol, 0.1 equiv), and a solution of ethyl glyoxylate (1.1 mmol, 1.1 equiv) in toluene (50% w/w) were mixed in EtOH (1.0 mL) and stirred at RT during 1 h until complete solubilization. The reaction was quenched with addition of a saturated $NaHCO_3$ solution (10 mL), and the product was extracted using dichloromethane (3 × 40 mL). The combined organic layers were washed with saturated brine (40 mL), dried over Na_2SO_4, filtrated, and the solvent was removed under reduced pressure to afford the corresponding ethyl glyoxylate oxime, which was pure enough to be engaged directly. Ethyl glyoxylate oxime (1.0 mmol, 1.0 equiv) was dissolved in EtOH (0.10 mL). BH_3.pyr (1.5 mmol, 1.5 equiv) was added to the mixture, which was cooled down to 0 °C. An ethanolic solution of HCl (6.0 M, 9.0 equiv, freshly prepared by addition of AcCl into EtOH at 0 °C) was added dropwise over a period of 3 h at 0 °C. After the addition of the acid, the mixture was stirred at RT for 30 min (the reaction completion was monitored by TLC until the disappearance of the ethyl glyoxylate oxime). Isolations of **6a** and **6b** were achieved as described below. Ethyl (benzyloxy)glycinate **6a:** The reaction was quenched with addition of an aqueous solution of NaOH (2.0 M) at 0 °C and the crude mixture was concentrated under reduced pressure to remove EtOH. The resulting oil was taken into dichloromethane and washed with water (3 × 40 mL). Combined organic layers were washed with saturated brine (3 × 20 mL), dried over Na_2SO_4, and filtrated, and the solvent was removed under reduced pressure to afford product **6a** as a yellowish oil (2.32 g, 11.1 mmol, 76% yield). R_f = 0.5 (hexanes/EtOAc 4:1 v/v); IR ν_{max}: 3068, 2923, 2854, 1685, 1451, 1231, 1121, 1002, 956, 758, 738 cm^{-1}; $^{13}C\{^1H\}$ NMR (100 MHz, $CDCl_3$, δ): 171.1, 137.8, 128.4 (3C), 127.9 (2C), 76.1, 61.1, 53.5, 14.2. Ethyl hydroxyglycinate **6b:** The crude mixture was concentrated under reduced pressure. The resulting oil was taken into dichloromethane and solid sodium carbonate was added to the solution at 0 °C. The mixture was then stirred overnight at room temperature. The solvent was filtrated and evaporated under reduced pressure to afford product **6b** as a yellowish oil (2.43 g, 20.4 mmol, 72% yield). R_f = 0.4 (hexanes/EtOAc 3:2 v/v); $^{13}C\{^1H\}$ NMR (100 MHz, $CDCl_3$, δ): 171.1, 61.2, 54.9, 14.2.

General Procedure A, for *N*-*O*-benzyl α-Amino Ester Coupling With *N*-Fmoc α-Amino Acids. Carboxylic acid **6a** (4.0 mmol, 4.0 equiv) and the secondary amine **Fmoc-AA-OH** (1.0 mmol, 1.0 equiv) were solubilized in CH_2Cl_2 and DMF (3:1; 4.0 mL). HOAt (4.4 mmol, 4.4 equiv) and HATU (4.0 mmol, 4.0 equiv) were added and the solution was stirred 10 min at RT. DIPEA (4.0 mmol, 4.0 equiv) was added to the mixture, which was stirred 4−15 h at RT. The reaction progress was monitored by TLC. CH_2Cl_2 (5.0 mL) was added and the reaction mixture was washed successively with a citric acid solution (10 mL, 5% w/w), saturated $NaHCO_3$ solution (10 mL), and saturated brine (10 mL). The organic layer was dried over Na_2SO_4, filtrated, and the solvent was evaporated under reduced pressure to afford the crude product **7a−c**, which was purified by chromatography.

*Fmoc-N(Me)-Gly-N(OBn)-Ethyl-Glycinate (**7a**).*

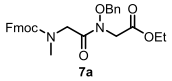

7a
$C_{29}H_{30}N_2O_6$
MW 502.21 g.mol^{-1}

was prepared according to the general procedure A, using ethyl *N*-(benzyloxy)glycinate **6a** (50 mg, 0.24 mmol, 1.0 equiv) and **Fmoc-Sar-OH** (149 mg, 0.48 mmol, 2.0 equiv). The crude product was purified by chromatography (hexanes/EtOAc 9:1 v/v) to afford **7a** in a pure form as a white foam (104 mg, 0.21 mmol, 87% yield). R_f = 0.6 (hexanes/EtOAc 1:1 v/v); mp 42−45 °C; IR ν_{max}: 2944, 1747, 1702, 1450, 1399, 1372, 1204, 1146, 992, 758, 739, 700 cm^{-1}; Product **7a** was characterized as a mixture of cis−trans rotamers in a ratio 2:3 by $^1H-^{13}C$ HSQC: ^1H NMR (400 MHz, $CDCl_3$, δ) trans rotamer: 7.77 (d, J = 7.5 Hz, 2H), 7.63 (d, J = 7.5 Hz, 2H), 7.40 (m, 5H), 7.34 (m, 4H), 4.93 (s, 2H), 4.39 (d, J = 7.0 Hz, 2H), 4.29 (s, 2H), 4.26 (s, 2H), 4.24 (t, J = 3.3 Hz, 1H), 4.21 (q, J = 7.1 Hz, 2H), 3.02 (s, 3H), 1.28 (t, J = 6.7 Hz, 3H); cis rotamer: 7.72 (d, J = 7.5 Hz, 2H), 7.56 (d, J = 7.5 Hz, 2H), 7.40 (m, 5H), 7.34 (m, 4H), 7.16 (m, 2H), 4.73 (s, 2H), 4.43 (d, J = 6.6 Hz, 2H), 4.29 (s, 2H), 4.24 (t, J = 3.3 Hz, 1H), 4.18 (q, J = 7.2 Hz, 2H), 4.07 (s, 2H), 2.91 (s, 2H), 1.25 (t, J = 7.1 Hz, 3H); $^{13}C\{^1H\}$ NMR (100 MHz, $CDCl_3$, δ) trans rotamer: 167.7 (2C), 157.0, 144.1 (2C), 141.3 (2C), 134.3, 129.6 (2C),129.2, 128.8 (2C), 127.6 (2C), 127.1 (2C), 125.2 (2C), 120.0 (2C), 77.3, 67.9, 61.7, 50.6, 49.9, 47.2, 35.6, 14.1; cis rotamer: 167.6 (2C), 156.4, 144.2 (2C), 141.3 (2C), 134.1, 129.6 (2C), 129.2, 128.8 (2C), 127.6 (2C), 127.1 (2C), 125.1 (2C), 119.9 (2C), 77.5, 67.3, 61.7, 50.3, 50.1, 47.3, 36.0, 14.1; HRMS-ESI (m/z): $[M + H]^+$ calcd for $C_{29}H_{31}N_2O_6$, 503.2177; found, 503.2161 (−3.2 ppm).

*Fmoc-Gly-N(OBn)-Ethyl-Glycinate (**7b**).*

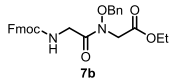

7b
$C_{28}H_{28}N_2O_6$
MW 488.19 g.mol^{-1}

was prepared according to the general procedure A, using ethyl *N*-(benzyloxy)glycinate **6a** (70 mg, 0.33 mmol, 1.0 equiv) and **Fmoc-Gly-OH** (398 mg, 1.34 mmol, 4.0 equiv). The crude product was purified by chromatography (hexanes/EtOAc 70:30 v/v) to afford **7b** in a pure form as a white foam (113 mg, 0.23 mmol, 70% yield). R_f = 0.2 (hexanes/EtOAc 70:30 v/v); mp 99−101 °C; IR ν_{max}: 3376, 2953, 1745, 1691, 1532, 1400, 1277, 1226, 992, 741, 730, 694 cm^{-1}; ^1H NMR (400 MHz, $CDCl_3$, δ): 7.77 (d, J = 7.5 Hz, 2H), 7.61 (d, J = 7.4 Hz, 2H), 7.40 (m, 7H), 7.32 (t, J = 7.3 Hz, 2H), 5.50 (br, 1H), 4.91 (s, 2H), 4.39 (d, J = 7.2 Hz, 2H), 4.28 (s, 2H), 4.22 (m, 5H), 1.27 (t, J = 7.1 Hz, 3H); $^{13}C\{^1H\}$ NMR (100 MHz, CD_3OD, δ): 173.1, 167.9, 157.7, 143.9 (2C), 141.2 (2C), 134.5, 129.4 (2C),128.8, 128.4 (2C), 127.4 (2C), 126.8 (2C), 124.9 (2C), 119.5 (2C), 76.9, 66.8, 61.3, 49.1, 47.1, 41.9, 13.0; HRMS-ESI (m/z): $[M + H]^+$ calcd for $C_{28}H_{29}N_2O_6$, 489.2020; found, 489.2013 (−1.4 ppm).

*Fmoc-Ile-N(OBn)-Ethyl-Glycinate (**7c**).*

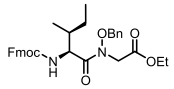

7c
$C_{32}H_{36}N_2O_6$
MW 544.26 g.mol^{-1}

was prepared according to the general procedure A, using ethyl *N*-(benzyloxy)glycinate **6a** (50 mg, 0.24 mmol, 1.0 equiv) and **Fmoc-Ile-OH** (298 mg, 0.96 mmol, 4.0 equiv). The crude product was purified by chromatography (hexanes/EtOAc 80:20 v/v) to afford **7c** in a pure form as a white foam (94 mg, 0.17 mmol, 72% yield). R_f = 0.4 (hexanes/EtOAc 70:30 v/v); mp 40−44 °C; **IR** ν_{max}: 3057, 2964, 1716, 1660, 1506, 1449, 1264, 1201, 1021, 732, 700 cm^{-1}; ^1H NMR (400 MHz, $CDCl_3$, δ): 7.47 (d, J = 7.5 Hz, 2H), 7.62 (d, J = 6.5 Hz, 2H), 7.41 (m, 7H), 7.32 (t, J = 7.4 Hz, 2H), 5.42 (d, J = 9.8 Hz, 1H), 5.05 (dd, J = 32.3, 10.1 Hz, 2H), 4.86 (dd, J = 9.7, 6.0 Hz, 1H), 4.64 (d, J = 17.4 Hz, 1H), 4.40 (m, 2H), 4.25 (t, J = 7.2 Hz, 1H), 4.20 (q, J = 7.1 Hz, 2H), 3.99 (d, J = 17.5 Hz, 1H), 1.95 (m, 1H), 1.60 (m, 1H), 1.26 (t, J = 7.1 Hz, 3H), 1.16 (m, 1H), 1.01 (d, J = 6.8 Hz, 3H), 0.91 (t, J = 7.4 Hz, 3H); $^{13}C\{^1H\}$ NMR (100 MHz, $CDCl_3$, δ): 174.0, 167.3, 156.5, 144.0, 143.9, 141.3 (2C), 133.9, 129.6 (2C),129.2, 128.8 (2C), 127.7 (2C), 127.1 (2C), 125.2 (2C), 120.0 (2C), 77.9, 67.1, 61.6, 55.4, 48.6, 47.2, 37.3, 23.9, 15.7, 14.1, 11.2; HRMS-ESI (m/z): $[M + H]^+$ calcd for $C_{32}H_{37}N_2O_6$, 545.2646; found, 545.2631 (−2.8 ppm).

General Procedure B, for the Coupling of 4 With *t*-butyl α-Amino Ester Residues. Carboxylic acid **4** (1.0 mmol, 1.0 equiv) and the **H-AA-O*t*Bu** (1.2 mmol, 1.2 equiv) were solubilized in CH_2Cl_2

https://dx.doi.org/10.1021/acs.joc.0c01441
J. Org. Chem. 2020, 85, 12329−12342

(5.0 mL) under an argon atmosphere and cooled down to 0 °C. EDCi (1.2 mmol, 1.2 equiv) and HOBt (1.2 mmol, 1.2 equiv) were added to the mixture. DIPEA (2.0 mmol, 2.0 equiv) was added to the mixture, which was stirred 15 h at RT. The reaction progress was monitored by TLC. CH_2Cl_2 (5.0 mL) was added and the mixture was washed successively with a citric acid solution (10 mL, 5% w/w), saturated $NaHCO_3$ solution (10 mL), and saturated brine (10 mL). The organic layer was dried over Na_2SO_4, filtrated, and the solvent was evaporated under reduced pressure to afford the crude product **11a,b**, which was purified by chromatography.

*Ac-N(OBn)-Gly-N(Me)-tert-Butyl-Glycinate (**11a**).*

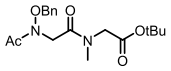

11a
$C_{18}H_{26}N_2O_5$
MW 350.18 g.mol^{-1}

was prepared according to the general procedure B, using *N*-acetyl-*N*-(benzyloxy)glycine **4** (100 mg, 0.45 mmol, 1.0 equiv) and **H-Sar-O*t*Bu** (98 mg, 0.54 mmol, 1.2 equiv). The crude product was purified by chromatography (ether/EtOAc 1:1 v/v) to afford **11a** in a pure form as an uncolored oil (106 mg, 0.30 mmol, 67% yield). R_f = 0.2 (hexanes/EtOAc 1:1 v/v); IR (dry film) ν_{max}: 2980, 2937, 2865, 1737, 1658, 1454, 1367, 1227, 1154, 1119, 1055, 1032, 1013, 846, 747, 700 cm^{-1}; Product **11a** was characterized as a mixture of cis−trans rotamers in a ratio 2:5 by ^{1}H−^{13}C HSQC: ^{1}H NMR (400 MHz, $CDCl_3$, δ) trans rotamer: 7.39 (m, 5H), 4.93 (s, 2H), 4.41 (s, 2H), 4.04 (s, 2H), 2.99 (s, 3H), 2.16 (s, 3H), 1.45 (s, 9H); cis rotamer: 7.39 (m, 5H), 4.93 (s, 2H), 4.33 (s, 2H), 3.91 (s, 2H), 2.98 (s, 3H), 2.14 (s, 3H), 1.48 (s, 9H); ^{13}C{^{1}H} NMR (100 MHz, $CDCl_3$, δ) trans rotamer: 175.1, 168.0, 167.2, 134.9, 129.5 (2C),128.9, 128.7 (2C), 82.0, 77.3, 50.3, 50.0, 35.6, 28.1, 20.4; cis rotamer: 175.1, 167.7, 167.4, 134.8, 129.5 (2C),128.9, 128.7 (2C), 82.9, 77.2, 52.1, 49.8, 35.4, 28.0 (3C), 20.4; HRMS-ESI (m/z): [M + H]$^+$ calcd for $C_{18}H_{27}N_2O_5$, 351.1914; found, 351.1911 (−0.9 ppm).

*Ac-N(OBn)-Gly-tert-Butyl-Glycinate (**11b**).*

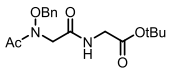

11b
$C_{17}H_{24}N_2O_5$
MW 336.17 g.mol^{-1}

was prepared according to the general procedure B, using *N*-acetyl-*N*-(benzyloxy)glycine **4** (500 mg, 2.24 mmol, 1.0 equiv) and **H-Gly-O*t*Bu** (376 mg, 2.69 mmol, 1.2 equiv). The crude product was purified by chromatography (hexanes/EtOAc 1:1 v/v) to afford **11b** in a pure form as a yellowish oil (604 mg, 1.80 mmol, 67% yield). R_f = 0.3 (hexanes/EtOAc 1:1 v/v); IR (dry film) ν_{max}: 3288, 2980, 2941, 2865, 1736, 1685, 1620, 1545, 1454, 1404, 1364, 1223, 1154, 1055, 1033, 1016, 961, 853, 753, 697, 641 cm^{-1}; ^{1}H NMR (400 MHz, $CDCl_3$, δ): 7.39 (s, 5H), 6.61 (br, 1H), 4.93 (s, 2H), 4.30 (s, 2H), 3.93 (d, J = 5.1 Hz, 2H), 2.14 (s, 3H), 1.46 (s, 9H); ^{13}C{^{1}H} NMR (100 MHz, $CDCl_3$, δ): 173.8, 168.5, 167.8, 134.1, 129.5 (2C),129.2, 128.8 (2C), 82.4, 77.4, 51.9, 42.0, 28.0 (3C), 20.3; HRMS-ESI (m/z): [M + H]$^+$ Calcd for $C_{17}H_{25}N_2O_5$, 337.1758; found, 337.1754 (−1.2 ppm).

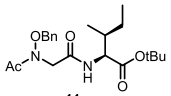

11c
$C_{21}H_{32}N_2O_5$
MW 392.23 g.mol^{-1}

*Ac-N(OBn)-Gly-tert-Butyl-Isoleucinate (**11c**).* *N*-acetyl-*N*-(benzyloxy)glycine **4** (700 mg, 3.14 mmol, 1.0 equiv), HATU (1.79 g, 4.71 mmol, 1.5 equiv), and HOAt (641 mg, 4.71 mmol, 1.5 equiv) were solubilized in DMF (8.0 mL) under an argon atmosphere. DIPEA (609 mg, 4.71 mmol, 1.5 equiv) was added to the mixture, which was preactivated 5 min at RT. **H-Ile-O*t*Bu** (1.40 g, 6.28 mmol, 2.0 equiv) was then added and stirred 15 h at RT. The reaction progress was monitored by TLC. CH_2Cl_2 (10 mL) was added and the mixture was washed successively with a citric acid solution (15 mL, 5% w/w), saturated $NaHCO_3$ solution (15 mL), and saturated brine (15 mL). The organic layer was dried over Na_2SO_4, filtrated, and the solvent was evaporated under reduced pressure to afford the crude product **11c** in a pure form as a yellow oily solid (841.5 mg, 2.1 mmol, 68% yield). R_f = 0.4 (hexanes/EtOAc 1:1 v/v); $[\alpha]_D^{18}$−21.7 (*c* 1.00, MeOH); IR (dry film) ν_{max}: 3358, 3276, 2962, 2932, 2873, 1735, 1720, 1689, 1650, 1556, 1536, 1448, 1412, 1391, 1365, 1287, 1257, 1151, 1133, 1079, 1028, 1009, 973, 948, 809, 737, 697 cm^{-1}; ^{1}H NMR (400 MHz, $CDCl_3$, δ): 7.38 (s, 5H), 6.66 (d, J = 8.1 Hz, 1H), 4.92 (s, 2H), 4.47 (dd, J = 8.5, 4.5 Hz, 1H), 4.34 (d, J = 16.5 Hz, 1H), 4.23 (d, J = 16.5 Hz, 1H), 2.14 (s, 3H), 1.87 (m, 1H), 1.58 (m, 1H), 1.45 (s, 9H), 1.15 (m, 1H), 0.92 (t, J = 7.4 Hz, 3H), 0.89 (d, J = 6.9 Hz, 3H); ^{13}C{^{1}H} NMR (100 MHz, $CDCl_3$, δ): 173.8, 170.5, 167.4, 134.1, 129.4 (2C),129.1, 128.8 (2C), 82.1, 77.2, 56.9, 52.0, 38.1, 28.1 (3C), 25.3, 20.3, 15.3, 11.7; HRMS-ESI (m/z): [M + Na]$^+$ calcd for $C_{21}H_{32}N_2O_5Na$, 415.2203; found, 415.2204 (+0.2 ppm).

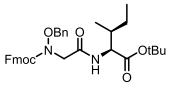

11d
$C_{34}H_{40}N_2O_6$
MW 572.29 g.mol^{-1}

*Fmoc-N(OBn)-Gly-tert-Butyl-Isoleucinate (**11d**).* N-Fmoc-N-(benzyloxy)glycine **5** (500 mg, 1.24 mmol, 1.0 equiv) and EEDQ (460 mg, 1.86 mmol, 1.5 equiv) were solubilized in CH_2Cl_2 (3.0 mL) under an argon atmosphere. The mixture was preactivated 5 min at RT. **H-Ile-O*t*Bu** (832 mg, 3.72 mmol, 3.0 equiv) was then added and stirred 5 h at RT. The reaction progress was monitored by TLC. CH_2Cl_2 (3.0 mL) was added and the mixture was washed successively with a citric acid solution (10 mL, 5% w/w), saturated $NaHCO_3$ solution (10 mL), and saturated brine (10 mL). The organic layer was dried over Na_2SO_4, filtrated, and the solvent was evaporated under reduced pressure to afford the crude product **11d** in a pure form as a yellow oily solid (618 mg, 1.08 mmol, 87% yield). R_f = 0.3 (hexanes/EtOAc 4:1 v/v); $[\alpha]_D^{18}$−10.1 (*c* 1.00, MeOH); **IR** (dry film) ν_{max}: 3343, 3067, 2965, 2936, 2880, 1725, 1685, 1523, 1451, 1414, 1392, 1368, 1340, 1249, 1216, 1143, 1092, 984, 912, 846, 757, 738, 698, 621 cm^{-1}; ^{1}H NMR (400 MHz, $CDCl_3$, δ): 7.75 (d, J = 7.5 Hz, 1H), 7.62 (m, 2H), 7.40 (t, J = 7.4 Hz, 2H), 7.32 (m, 7H), 6.55 (d, J = 8.4 Hz, 1H), 4.85 (s, 2H), 4.59 (dd, J = 6.6, 2.8 Hz, 2H), 4.48 (dd, J = 8.5, 4.5 Hz, 1H), 4.28 (t, J = 6.6 Hz, 1H), 4.14 (d, J = 17.2 Hz, 1H), 4.03 (d, J = 17.2 Hz, 1H), 1.84 (m, 1H), 1.42 (s, 9H), 1.40 (m, 1H), 1.11 (m, 1H), 0.86 (m, 6H); ^{13}C{^{1}H} NMR (100 MHz, $CDCl_3$, δ): 170.5, 167.4, 157.5, 143.5 (2C), 141.4 (2C) 134.9, 129.4 (2C),128.7, 128.5 (2C), 127.8 (2C), 127.2 (2C), 125.1 (2C), 120.0 (2C), 82.1, 77.2, 68.3, 56.8, 54.3, 47.1, 38.2, 28.0 (3C), 25.3, 15.3, 11.7; HRMS-ESI (m/z): [M + Na]$^+$ calcd for $C_{34}H_{40}N_2O_6Na$, 595.2779; found, 595.2763 (−2.7 ppm).

*General Procedure C, for the Coupling of **6a** or **6b** With **11a−c**.* *t*-Butyl protected dipeptide **11a−c** (1.0 mmol, 1.0 equiv) was solubilized in dichloromethane (5.0 mL) and cooled down to 0 °C. Trifluoroacetic acid (5.0 mL) was added dropwise, the mixture was then stirred at 0 °C for 3−5 h. The reaction progress was monitored by TLC. The solvent and residual byproducts were evaporated under reduced pressure to afford the desired unprotected acid dimer. The resulting product and the ethyl (benzyloxy)glycinate **6a** or ethyl hydroxyglycinate **6b** (2.0 mmol, 2.0 equiv) were solubilized in CH_2Cl_2 or DMF (5.0 mL). Then, HOAt (2.0 mmol, 2.0 equiv) and HATU (2.0 mmol, 2.0 equiv) were added, and the solution was stirred 10 min at RT. DIPEA (2.0 mmol, 2.0 equiv) was added dropwise to the mixture, which was stirred 15 h at RT. The reaction progress was monitored by TLC. CH_2Cl_2 (5.0 mL) was added and the mixture was washed successively with a citric acid solution (10 mL, 5% w/w), saturated $NaHCO_3$ solution (10 mL), and saturated brine (10 mL). The organic layer was dried over Na_2SO_4, filtrated, and the solvent was evaporated under reduced pressure to afford crude products **9a−d**, which were further purified by chromatography.

https://dx.doi.org/10.1021/acs.joc.0c01441
J. Org. Chem. 2020, 85, 12329−12342

*Ac-N(OBn)-Gly-N(Me)-Gly-N(OBn)-Ethyl-Glycinate (**9a**).*

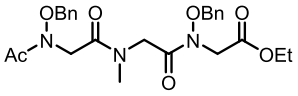

9a

$C_{25}H_{31}N_3O_7$

MW 485.22 g.mol^{-1}

was prepared according to the general procedure C, using *N*-(benzyloxy)glycinate **6a** (740 mg, 3.54 mmol, 2.0 equiv) and peptide **11a** (520 mg, 1.77 mmol, 1.0 equiv). The crude product was purified by chromatography (hexanes/EtOAc 7:3 v/v) to afford **9a** as a white foam (277 mg, 0.57 mmol, 32% yield). R_f = 0.3 (hexanes/EtOAc 3:7 v/v); mp 47−49 °C; IR ν_{max}: 2931, 1743, 1658, 1454, 1373, 1204, 1021, 973, 844, 733, 700 cm^{-1}; Product **9a** was characterized as a mixture of cis−trans rotamers in a ratio 1:2 by ^{1}H−^{13}C HSQC: ^{1}H NMR (400 MHz, $CDCl_3$, δ) trans rotamer: 7.38 (m, 5H), 4.92 (s, 2H), 4.91 (s, 2H), 4.42 (s, 2H), 4.38 (s, 2H), 4.23 (s, 2H), 4.18 (m, 2H), 2.97 (s, 3H), 2.16 (s, 3H), 1.26 (t, J = 7.1 Hz, 3H); cis rotamer: 7.38 (m, 5H), 4.88 (s, 2H), 4.84 (s, 2H), 4.33 (s, 2H), 4.18 (m, 4H), 3.98 (br, 2H), 2.80 (s, 3H), 2.10 (s, 3H), 1.26 (t, J = 7.1 Hz, 3H); ^{13}C{^{1}H} NMR (100 MHz, $CDCl_3$, δ) trans rotamer: 175.0, 172.3, 167.7, 167.5, 134.9, 134.2, 129.6 (2C), 129.5 (2C), 129.2, 129.0, 128.8 (2C), 128.7 (2C) 77.6 (2C), 61.6, 50.1 (2C), 49.6, 35.9, 20.4, 14.1; cis rotamer: 175.0, 173.3, 167.8, 167.4, 134.9, 134.1, 130.1 (2C), 129.6 (2C), 128.9, 128.8 (2C), 128.7, 128.5 (2C), 82.9, 77.0, 76.9, 61.9, 51.0, 50.1, 49.2, 35.4, 20.3, 14.1; HRMS-ESI (m/z): [M + H]$^+$ calcd for $C_{25}H_{32}N_3O_7$, 486.2235; found 486.2214 (−4.3 ppm).

*Ac-N(OBn)-Gly-Gly-N(OBn)-Ethyl-Glycinate (**9b**).*

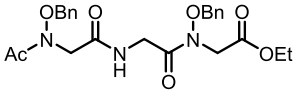

9b

$C_{24}H_{29}N_3O_7$

MW 471.20 g.mol^{-1}

was prepared according to the general procedure C, using *N*-(benzyloxy)glycinate **6a** (242 mg, 1.16 mmol, 2.0 equiv) and peptide **11b** (171 mg, 0.58 mmol, 1.0 equiv). The crude product was purified by precipitation into petroleum ether and filtration to afford **9b** as a beige solid (127 mg, 0.27 mmol, 46% yield). R_f = 0.3 (hexanes/EtOAc 3:7 v/v); mp 91−96 °C; IR ν_{max}: 3239, 2979, 2953, 1745, 1695, 1674, 1644 1544, 1455, 1403, 1372, 1240, 1207, 1054, 1033, 1007, 972, 737 cm^{-1}; ^{1}H NMR (400 MHz, $CDCl_3$, δ): 7.38 (s, 10H), 6.76 (br, 1H), 4.91 (d, J = 10.7 Hz, 2H), 4.29 (s, 2H), 4.26 (d, J = 4.6 Hz, 2H), 4.24 (s, 2H), 4.18 (q, J = 7.2 Hz, 2H), 2.15 (s, 3H), 1.25 (t, J = 7.2 Hz, 3H); ^{13}C{^{1}H} NMR (100 MHz, $CDCl_3$, δ): 174.1, 172.5, 167.8, 167.3, 134.2, 133.9, 129.5 (4C),129.3, 129.1, 128.9 (2C), 128.8 (2C), 77.8, 77.5, 61.8, 51.8, 50.0, 41.3, 20.4, 14.1; HRMS-ESI (m/z): [M + H]$^+$ Calcd for $C_{24}H_{30}N_3O_7$, 472.2078; found, 472.2061 (−3.6 ppm).

*Ac-N(OBn)-Gly-Ile-N(OBn)-Ethyl-Glycinate (**9c**).*

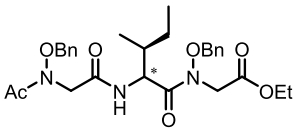

9c

$C_{28}H_{37}N_3O_7$

MW 527.26 g.mol^{-1}

was prepared according to the general procedure C, using *N*-(benzyloxy)glycinate **6a** (363 mg, 1.74 mmol, 2.0 equiv) and peptide **11c** (292 mg, 0.87 mmol, 1.0 equiv). The crude product was purified by precipitation into petroleum ether and filtration to afford **9c** as an orange powder in a mixture of diastereoisomer (189 mg, 0.44 mmol, 41% yield, d.r. 3:2). R_f = 0.7 (hexanes/EtOAc 3:7 v/v); mp 117−120 °C; **IR** ν_{max}: 3279, 2964, 2933, 1751, 1637, 1544, 1454, 1390, 1375, 1212, 1019, 972, 840, 750, 699 cm^{-1}; ^{1}H NMR (400 MHz, $CDCl_3$, δ) (*S, S*) isomer: 7.44 (m, 10H), 6.88 (d, J = 9.3 Hz, 1H), 5.10 (dd, J = 9.3, 6.7 Hz, 1H), 5.00 (m, 2H), 4.93 (s, 2H), 4.58 (d, J = 8.3 Hz, 1H), 4.33 (d, J = 3.5 Hz, 2H), 4.17 (m, 3H), 2.12 (s, 3H), 1.90 (m, 1H), 1.55 (m, 1H), 1.24 (t, J = 7.1 Hz, 3H), 1.13 (m, 1H), 0.94 (d, J = 6.9 Hz, 3H), 0.86 (m, 3H); (*R, S*) isomer: 7.44 (m, 10H), 6.83 (d, J = 8.9 Hz, 1H), 5.19 (dd, J = 9.3, 4.3 Hz, 1H), 5.01 (s, 2H), 5.00 (m, 2H), 4.63 (d, J = 8.4 Hz, 1H), 4.33 (d, J = 3.5 Hz, 2H), 4.17 (m, 3H), 2.12 (s, 3H), 1.97 (m, 1H), 1.39 (m, 1H), 1.24 (t, J = 7.1 Hz, 3H), 1.20 (m, 1H), 0.87 (m, 3H), 0.84 (m, 3H); ^{13}C{^{1}H} NMR (100 MHz, $CDCl_3$, δ) (*S, S*) isomer: 173.7, 172.9, 167.7, 167.4, 135.0, 134.4, 129.7 (2C),129.6 (2C), 128.8, 128.7 (2C), 128.6 (2C), 77.2, 76.5, 61.3, 53.0, 50.2, 48.1, 36.9, 23.9, 19.8, 15.0, 13.5, 10.4; (*R, S*) isomer: 173.7, 173.2, 167.7, 167.6, 135.0, 134.3, 129.7 (2C),129.6 (2C), 129.0, 128.7 (2C), 128.6 (2C), 77.1, 76.5, 61.3, 51.9, 50.2, 48.2, 36.3, 26.4, 19.8, 15.0, 13.5, 11.1; HRMS-ESI (m/z): [M + H]$^+$ calcd for $C_{28}H_{38}N_3O_7$, 528.2704; found, 528.2681 (−4.4 ppm).

*Ac-N(OBn)-Gly-Ile-N(OH)-Ethyl-Glycinate (**9c′**).*

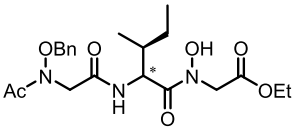

9c'

$C_{21}H_{31}N_3O_7$

MW 437.22 g.mol^{-1}

was prepared according to the general procedure C, using *N*-hydroxyglycinate **6b** (283 mg, 2.38 mmol, 2.0 equiv) and peptide **11c** (400 mg, 1.19 mmol, 1.0 equiv). The crude product was purified by precipitation into petroleum ether and filtration to afford **9c′** as a light brown solid (231 mg, 0.53 mmol, 53% yield). R_f = 0.4 (hexanes/EtOAc 3:7 v/v); $[\alpha]_D^{18}$−14.1 (*c* 1.00, MeOH); mp 118−120 °C; IR ν_{max}: 3280, 2968, 2934, 1753, 1655, 1637, 1541, 1372, 1245, 1201, 1018, 737, 696, 621 cm^{-1}; ^{1}H NMR (400 MHz, CD_3CN, δ): 8.38 (s, 1H), 7.43 (m, 5H), 6.88 (d, J = 8.9 Hz, 1H), 4.97 (dd, J = 9.1, 6.5 Hz, 1H), 4.92 (s, 2H), 4.44 (d, J = 17.5 Hz, 1H), 4.29 (d, J = 2.1 Hz, 2H), 4.25 (d, J = 17.5 Hz, 1H), 4.17 (q, J = 7.0 Hz, 2H), 2.11 (s, 3H), 1.97 (m, 1H), 1.52 (m, 1H), 1.24 (t, J = 7.1 Hz, 3H), 1.11 (m, 1H), 0.94 (d, J = 6.9 Hz, 3H), 0.90 (t, J = 7.4 Hz, 3H); ^{13}C{^{1}H} NMR (100 MHz, CD_3CN, δ): 173.8, 171.9, 167.9, 167.7, 134.9, 129.6 (2C),128.8, 128.6 (2C), 76.5, 61.2, 53.3, 50.1 (2C), 36.5, 23.8, 19.7, 15.1, 13.5, 10.6; HRMS-ESI (m/z): [M + H]$^+$ calcd for $C_{21}H_{32}N_3O_7$, 438.2235; found, 438.2214 (−4.8 ppm).

*Fmoc-N(OBn)-Gly-Ile-N(OBn)-Ethyl-Glycinate (**9d**).*

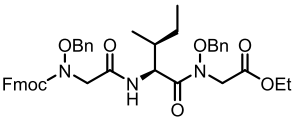

9d

$C_{41}H_{45}N_3O_8$

MW 707.32 g.mol^{-1}

Peptide **11d** (190 mg, 0.37 mmol, 1.0 equiv), lutidine (0.03 mL, 0.44 mmol, 1.2 equiv), and **6a** (308 mg, 1.47 mmol, 4.0 equiv) were solubilized in CH_2Cl_2 (1.0 mL) under an argon atmosphere. ClCO*t*Bu (0.05 mL, 0.44 mmol, 1.2 equiv) was then added and stirred 15 h at RT. The reaction progress was monitored by TLC. CH_2Cl_2 (3.0 mL) was added and the mixture was washed successively with a citric acid solution (3 × 5.0 mL, 5% w/w), saturated $NaHCO_3$ solution (3 × 5.0 mL), and saturated brine (5.0 mL). The organic layer was dried over Na_2SO_4, filtrated, and the solvent was evaporated under reduced pressure to afford the crude product **9d** in a pure form as a yellowish oily gum (135 mg, 0.19 mmol, 51% yield). R_f = 0.65 (hexanes/EtOAc 6:4 v/v); $[\alpha]_D^{18}$−7.8 (*c* 1.00, MeOH); IR ν(dry film) ν_{max}: 3320, 2961, 2934, 2876, 1743, 1712, 1655, 1526, 1451, 1419, 1389, 1344, 1200, 1094, 1022, 979, 911, 854, 739, 698 cm^{-1}; ^{1}H NMR (400 MHz, $CDCl_3$, δ) 7.75 (d, J = 7.5 Hz, 2H), 7.64 (dd, J = 7.3, 2.4 Hz, 2H), 7.37 (m, 14H), 6.59 (d, J = 9.4 Hz, 1H), 5.15 (dd, J = 9.4, 5.9 Hz, 1H), 5.03 (d, J = 10.1 Hz, 1H), 4.93 (d, J = 10.1 Hz, 1H), 4.86 (dd, J = 13.6, 10.1 Hz, 2H), 4.59 (m, 3H), 4.29 (m, 1H), 4.16 (m, 3H), 4.06 (d, J = 17.1 Hz, 1H), 3.90 (d, J = 17.5 Hz, 1H), 1.92 (m, 1H), 1.52 (m, 1H), 1.23 (t, J = 7.1 Hz, 3H), 1.03 (m, 1H), 0.95 (d, J = 6.8 Hz, 3H), 0.82 (t, J = 7.4 Hz, 3H); ^{13}C{^{1}H} NMR

https://dx.doi.org/10.1021/acs.joc.0c01441
J. Org. Chem. 2020, 85, 12329−12342

(100 MHz, $CDCl_3$, δ) 173.3, 167.8, 167.3, 157.7, 143.6 (2C), 141.4 (2C), 135.0, 133.9, 129.6 (2C), 129.4 (2C), 129.1, 128.8, 128.7, 128.5 (2C), 127.8 (2C), 127.2 (2C), 125.2 (2C), 120.0 (2C), 77.9, 77.5, 68.3, 61.6, 54.3, 53.3, 48.5, 47.1, 37.2, 23.9, 15.7, 14.1, 11.1; HRMS-ESI (m/z): $[M + Na]^+$ calcd for $C_{31}H_{45}N_3O_8Na$, 730.3099; found, 730.3087 (−1.6 ppm).

General Procedure D, for the Catalytic Hydrogenation of *N*-(benzyloxy)-Protecting Groups. Peptides **9a−d** (1.0 mmol, 1.0 equiv) were solubilized in EtOH (10 mL) and Pd/C (0.10 mmol, 0.10 equiv, 10% w/w) was added to the solution. For **9d**, the mixture was cooled down to 0 °C. The flask was placed under an atmosphere of a balloon of $H_{2,gas}$ and the mixture was stirred for 1−18 h (reaction progress monitored by TLC). The reaction mixture was filtered through a pad of cleaned Celite with silica (1% w/w), and the solvent was evaporated to afford the crude product **12a−d**, which were further purified by chromatography.

*Ac-N(OH)-Gly-N(Me)-Gly-N(OH)-Ethyl-Glycinate (**12a**).*

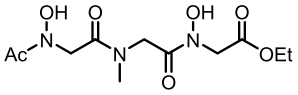

12a

$C_{11}H_{19}N_3O_7$

MW 305.12 g.mol^{-1}

was prepared according to the general procedure D, using peptide **9a** (63 mg, 0.13 mmol, 1.0 equiv). The crude product was purified by chromatography (gradient of hexanes/EtOAc 1:1 to EtOAc 100% and then EtOAc/MeOH 19:1) to afford **12a** in a pure form as an uncolored oil (32 mg, 0.11 mmol, 81% yield). R_f = 0.10 (hexanes/EtOAc/AcOH 5:4:1); mp 118−121 °C; IR ν_{max}: 3433, 3193, 2924, 2852, 1741, 1636, 1460, 1401, 1208, 1124, 1023, 822, 562 cm^{-1}; product **12a** was characterized as a mixture of cis−trans rotamers in a ratio 2:3 by $^1H-^{13}C$ HSQC: ^1H NMR (400 MHz, DMSO-d_6, δ) trans rotamer: 10.18 (s, 1H), 9.76 (s, 1H), 4.42 (s, 2H), 4.29 (s, 2H), 4.28 (s, 2H), 4.13 (q, J = 7.1 Hz, 2H), 2.93 (s, 3H), 2.02 (s, 3H), 1.20 (t,, J = 7.1 Hz, 3H); cis rotamer: 10.23 (s, 1H), 9.72 (s, 1H), 4.34 (s, 2H), 4.33 (s, 2H), 4.24 (s, 2H), 4.13 (q, J = 7.1 Hz, 2H), 2.81 (s, 3H), 2.02 (s, 3H), 1.20 (t,, J = 7.1 Hz, 3H); $^{13}C\{^1H\}$ NMR (100 MHz, $CDCl_3$, δ) trans rotamer: 172.8, 169.9, 169.6, 168.5, 61.9, 50.1, 49.5, 49.0, 36.4, 20.0, 14.1; cis rotamer: 172.8, 170.4, 169.4, 168.2, 61.9, 50.6, 50.5, 49.1, 35.4, 19.9, 14.1; HRMS-ESI (m/z): $[M + Na]^+$ calcd for $C_{11}H_{19}N_3O_7Na$, 328.1115; found, 328.1101 (−4.2 ppm).

*Ac-N(OH)-Gly-Gly-N(OH)-Ethyl-Glycinate (**12b**).*

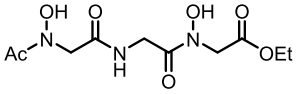

12b

$C_{10}H_{17}N_3O_7$

MW 291.11 g.mol^{-1}

was prepared according to the general procedure D, using peptide **9b** (170 mg, 0.36 mmol, 1.0 equiv). The crude product was purified by chromatography (gradient of hexanes/EtOAc 1:1 to EtOAc 100% and then EtOAc/MeOH 19:1) to afford **12b** in a pure form as a white solid (82 mg, 0.28 mmol, 79% yield). R_f = 0.05 (hexanes/EtOAc/AcOH 5:4:1); mp 140−142 °C; IR ν_{max}: 3299, 3097, 2911, 2778, 2680, 1743, 1678, 1646, 1593, 1564, 1464, 1411, 1388, 1376, 1257, 1218, 1189, 1027, 823, 786, 729, 615, 541 cm^{-1}; ^1H NMR (400 MHz, DMSO-d_6, δ): 10.21 (s, 1H), 9.91 (s, 1H), 8.00 (br, 1H), 4.30 (s, 2H), 4.17 (s, 2H), 4.12 (q, J = 7.1 Hz, 2H), 4.08 (d, J = 5.6 Hz, 2H), 2.02 (s, 3H), 1.20 (t, J = 7.1 Hz, 3H); $^{13}C\{^1H\}$ NMR (100 MHz, DMSO-d_6, δ): 171.9, 170.9, 168.3, 168.0, 61.3, 51.4, 51.1, 40.4, 20.6, 14.5; HRMS-ESI (m/z): $[M + Na]^+$ calcd for $C_{10}H_{17}N_3O_7Na$, 314.0959; found, 314.0958 (+0.3 ppm).

*Ac-N(OH)-Gly-Ile-N(OH)-Ethyl-Glycinate (**12c**).*

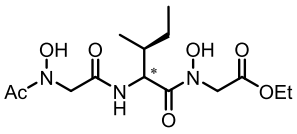

12c

$C_{14}H_{25}N_3O_7$

MW 347.17 g.mol^{-1}

was prepared according to the general procedure D, using peptide **9c′** (300 mg, 0.69 mmol, 1.0 equiv). The crude product was purified by chromatography (gradient of hexanes/EtOAc 1:1 to EtOAc 100% and then EtOAc/MeOH 19:1) to afford **12c** in a pure form as a yellow solid (239 mg, 0.69 mmol, 99% yield). R_f = 0.54 (hexanes/EtOAc/AcOH 5:4:1); $[\alpha]_D^{18}$−14.2 (c 1.00, MeOH); mp 97−99 °C; IR ν_{max}: 3276, 3210, 2965, 2−934, 1743, 1629, 1534, 1456, 1375, 1201, 1022, 634, 557 cm^{-1}; ^1H NMR (400 MHz, DMSO-d_6, δ): 10.24 (s, 1H), 9.89 (s, 1H), 7.82 (d, 1H), 5.02 (dd, J = 9.1, 6.0 Hz, 1H), 4.52 (d, J = 17.3 Hz, 1H), 4.18 (s, 2H), 4.12 (q, J = 7.0 Hz, 2H), 4.08 (d, J = 17.4 Hz, 1H), 2.01 (s, 3H), 1.87 (m, 1H), 1.44 (m, 1H), 1.19 (t, J = 7.1 Hz, 3H), 1.05 (m, 1H), 0.87 (d, J = 6.8 Hz, 3H), 0.83 (t, J = 7.3 Hz, 3H); $^{13}C\{^1H\}$ NMR (100 MHz, $CDCl_3$, δ): 173.5, 172.2, 169.8, 168.0, 61.8, 53.6, 51.4, 50.0, 36.0, 24.4, 20.1, 15.4, 14.1, 11.0; HRMS-ESI (m/z): $[M + H]^+$ calcd for $C_{25}H_{31}N_2O_6$, 348.1765; found, 348.1766 (+0.3 ppm).

*Fmoc-N(OH)-Gly-Ile-N(OH)-Ethyl-Glycinate (**12d**).*

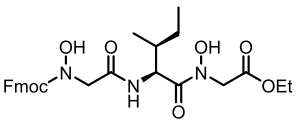

12d

$C_{27}H_{33}N_3O_8$

MW 527.23 g.mol^{-1}

was prepared according to the general procedure D, using peptide 9d (15 mg, 0.02 mmol, 1.0 equiv). The crude product was purified by chromatography (gradient of hexanes/EtOAc 4:1 to 2:6) to afford 12d in a pure form as a white powder (7 mg, 0.01 mmol, 62% yield). R_f = 0.38 (hexanes/EtOAc 2:3 v/v); $[\alpha]_D^{18}$−2.6 (c 0.50, MeOH); mp 164−169 °C; IR ν_{max}: 3284, 2961, 2923, 2873, 1745, 1711, 1685, 1610, 1541, 1449, 1401, 1376, 1352, 1213, 1111, 1020, 974, 942, 738, 621 cm^{-1}; ^1H NMR (400 MHz, DMSO-d_6, δ) 10.26 (s, 1H), 9.69 (s, 1H), 7.89 (d, J = 7.8 Hz, 3H), 7.70 (d, J = 7.5 Hz, 2H), 7.42 (t, J = 7.5 Hz, 2H), 7.32 (t, J = 7.5 Hz, 2H), 5.06 (dd, J = 9.3, 5.9 Hz, 1H), 4.51 (d, J = 17.3 Hz, 1H), 4.26 (m, 3H), 4.13 (m, 5H), 1.88 (m, 1H), 1.45 (m, 1H), 1.18 (t, J = 7.1 Hz, 3H), 1.06 (m, 1H), 0.88 (d, J = 6.8 Hz, 3H), 0.82 (t, J = 7.2 Hz, 3H); $^{13}C\{^1H\}$ NMR (100 MHz, $CDCl_3$, δ) 172.0, 169.9, 168.1, 158.1, 143.5 (2C), 141.3 (2C), 127.8 (2C),127.2 (2C), 125.2 (2C), 120.0 (2C), 68.9, 61.8, 54.4, 53.4, 49.9, 46.9, 35.8, 24.6, 15.4, 14.0, 10.9; HRMS-ESI (m/z): $[M + Na]^+$ calcd for $C_{27}H_{33}N_3O_8Na$, 550.2160; found, 550.2163 (+0.5 ppm).

*N-(((9H-Fluoren-9-yl)methoxy)carbonyl)-N-benzylglycine (**SI-1**).*

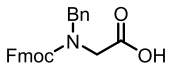

SI-1

$C_{24}H_{21}NO_4$

MW 387.15 g.mol^{-1}

Benzylamine (200 mg, 1.87 mmol, 1.0 equiv) and glyoxylic acid monohydrate (344 mg, 3.73 mmol, 2.0 equiv) were solubilized in CH_2Cl_2 (9.0 mL) and stirred overnight at RT. The solvent was then evaporated and the *N*-benzyl-*N*-formylglycine intermediate was characterized by ^1H NMR (400 MHz, DMSO-d_6, δ): 8.31 (s, 1H), 7.35 (m, 5H), 4.50 (s, 2H), and 3.83 (s, 2H). The crude *N*-benzyl-*N*-formylglycine was solubilized in a 1.0 M aqueous solution of HCl (9.0 mL) and stirred at reflux overnight. The water was then evaporated under reduced pressure to afford the desired *N*-benzylglycine hydrochloride (203 mg, 1.0 mmol, 54% yield) as a brown solid, which was used without any purification for the second step. R_f = 0.7

https://dx.doi.org/10.1021/acs.joc.0c01441
J. Org. Chem. 2020, 85, 12329−12342

(CH_2Cl_2/MeOH/AcOH 16:3:1 v/v); *N*-benzylglycine hydrochloride (200 mg, 0.99 mmol, 1.0 equiv) was solubilized in dioxane (6.0 mL) and the solution was cooled down to 0 °C. A solution of sodium bicarbonate (200 mg, 2.44 mmol, 2.4 equiv) in water (2.0 mL) was then added and the mixture was stirred for 10 min at 0 °C. A solution of (9*H*-fluoren-9-yl)methyl chloroformate (471 mg, 1.82 mmol, 1.8 equiv) in dioxane (2.0 mL) was added to the mixture, which was slowly warm to RT and stirred overnight. Water was added and the aqueous layer (pH ∼ 8) was washed with ethyl acetate (2 × 15 mL). The aqueous layer was acidified with a 5.0 M aqueous solution of HCl to pH ∼ 3. The product was extracted with ethyl acetate (3 × 15 mL), the combined organic layers were dried over Na_2SO_4, filtrated, and the solvent was evaporated under reduced pressure. The crude product was purified by flash chromatography (isocratic solvent mixture of hexanes/EtOAc, 4:1 v/v) to afford product **SI-1** in a pure form as a white powder (107 mg, 0.28 mmol, 28% yield over 3 steps). R_f = 0.7 (100% EtOAc); mp 110.0−113.0 (±0.6) °C; IR ν_{max}: 3068, 2923, 2854, 1685, 1451, 1231, 1121, 1002, 956, 758, 738 cm^{-1}; Product **SI-1** was characterized as a mixture of cis−trans rotamers in a 1:1 ratio by $^1H-^{13}C$ HSQC: ^1H NMR (400 MHz, CD_3OD, δ) trans rotamer: 7.77 (d, J = 7.5 Hz, 2H), 7.50 (d, J = 7.5 Hz, 2H), 7.34 (t, J = 5.9 Hz, 2H), 7.23 (m, 5H), 6.96 (m, 2H), 4.53 (d, J = 5.8 Hz, 2H), 4.32 (s, 2H), 4.22 (t, J = 5.8 Hz, 1H), 3.85 (s, 2H); *cis* rotamer: 7.73 (d, J = 7.5 Hz, 2H), 7.59 (d, J = 7.5 Hz, 2H), 7.37 (t, J = 5.8 Hz, 2H), 7.29 (m, 5H), 7.16 (m, 2H), 4.49 (s, 2H), 4.47 (d, J = 6.3 Hz, 2H), 4.22 (t, J = 5.8 Hz, 1H), 3.73 (s, 2H).

*Ethyl Benzylglycinate (**SI-2**).*

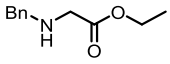

SI-2
$C_{11}H_{15}NO_2$
MW 193.11 g.mol^{-1}

Benzylamine (1.00 g, 9.33 mmol, 1.0 equiv) and a solution of ethyl glyoxylate (1.05 g, 10.3 mmol, 1.1 equiv) in toluene (50% w/w) were solubilized in dry ethanol (19.0 mL) and stirred for 1 h at RT. A solution of sodium cyanoborohydride (1.18 g, 18.7 mmol, 2.0 equiv) in dry ethanol (3.0 mL) and acetic acid (0.05 mL, 0.93 mmol, 0.1 equiv) were added to the mixture, which was stirred overnight at RT. The reaction completion was monitored by TLC (R_f = 0.35, EtOAc/hexanes 1:1 v/v). The solvent was then evaporated and the crude was solubilized in dichloromethane (10 mL). The organic layer was washed with water (3 × 10 mL), dried over Na_2SO_4, and filtrated, and the solvent was evaporated under reduced pressure. The crude product was purified by chromatography (isocratic solvent mixture of hexanes/EtOAc, 7:3 v/v) to afford **SI-2** in a pure form as a yellow oil (542 mg, 2.81 mmol, 30% yield). R_f = 0.3 (EtOAc/hexanes 1:1 v/v); IR ν_{max}: 3029, 2980, 2866, 1724, 1453, 1371, 1188, 1142, 1025, 736, 698 cm^{-1}.

*Fmoc-Ile-N(OH)-Ethyl-Glycinate (**SI-3**).*

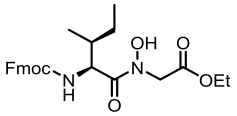

SI-3
$C_{25}H_{30}N_2O_6$
MW 454.21 g.mol^{-1}

was prepared according to the general procedure D, using peptide **7c** (450 mg, 0.83 mmol, 1.0 equiv). The crude product was purified by chromatography (hexanes/EtOAc 7:3 v/v) to afford **SI-3** in a pure form as a white solid (339 mg, 0.75 mmol, 90% yield). R_f = 0.3 (hexanes/EtOAc 7:3 v/v); $[\alpha]_D^{18}$−14.8 (c 1.00, MeOH); mp 147−149 °C; **IR** ν_{max}: 3325, 3144, 2968, 1741, 1692, 1605, 1530, 1449, 1211, 1023, 758, 737, 646, 621 cm^{-1}; ^1H NMR (400 MHz, $CDCl_3$, δ): 8.35 (br, 1H), 7.75 (d, J = 7.5 Hz, 2H), 7.56 (dd, J = 7.3, 2.9 Hz, 2H), 7.39 (t, J = 7.5 Hz, 2H), 7.29 (t, J = 7.4 Hz, 2H), 5.53 (d, J = 9.1 Hz, 1H), 4.82 (t, J = 8.4 Hz, 1H), 4.45 (s, 2H), 4.37 (m, 2H), 4.20 (m, 3H), 1.94 (m, 1H), 1.61 (m, 1H), 1.25 (t, J = 7.1 Hz, 3H), 1.20 (m, 1H), 1.00 (d, J = 6.7 Hz, 3H), 0.93 (t, J = 7.3 Hz, 3H); $^{13}C\{^1H\}$ NMR (100 MHz, $CDCl_3$, δ): 172.5, 168.4, 157.2, 143.8, 143.7, 141.3 (2C), 127.7 (2C), 127.1 (2C), 125.1 (2C), 120.0 (2C), 67.5, 61.8, 55.4, 49.4, 47.1, 36.4, 24.4, 15.6, 14.1, 11.1; HRMS-ESI (m/z): $[M + H]^+$ calcd for $C_{25}H_{31}N_2O_6$, 455.2177; found, 455.2157 (−4.4 ppm).

*Ac-N(OH)-Gly-tert-Butyl-Isoleucinate (**SI-4**).*

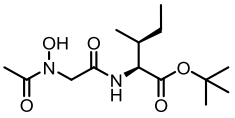

SI-4
$C_{14}H_{26}N_2O_5$
MW 302.18 g.mol^{-1}

was prepared according to the general procedure D, using peptide **11c** (450 g, 1.15 mmol, 1.0 equiv). The crude product was purified by chromatography (hexanes/EtOAc 6:4 v/v) to afford **SI-4** in a pure form as an uncolored oil (344 g, 1.14 mmol, 99% yield). R_f = 0.2 (hexanes/EtOAc 6:4 v/v); $[\alpha]_D^{18}$−15.1 (c 1.00, MeOH); IR (dry film) ν_{max}: 3268, 2967, 2934, 1732, 1659, 1637, 1536, 1458, 1393, 1367, 1248, 1142, 1038, 989, 846, 776, 582 cm^{-1}; ^1H NMR (400 MHz, DMSO-d_6, δ): 9.87 (s, 1H), 6.02 (d, J = 8.4 Hz, 1H), 4.17 (m, 3H), 2.01 (s, 3H), 1.74 (m, 1H), 1.41 (s, 3H), 1.37 (m, 1H), 1.18 (m, 1H), 0.86 (m, 6H); $^{13}C\{^1H\}$ NMR (100 MHz, DMSO-d_6, δ): 171.9, 170.9, 167.6, 81.2, 57.1, 51.2, 37.3, 28.1 (3C), 25.3, 20.6, 15.9, 11.8; HRMS-ESI (m/z): $[M + Na]^+$ calcd for $C_{14}H_{26}N_2O_5Na$, 325.1734; found, 325.1732 (−0.6 ppm).

*Ga(Fmoc-Ile-N(O)-Ethyl-Glycinate)$_3$ (**SI-5**).*

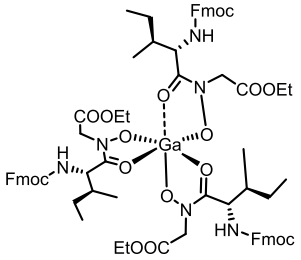

SI-5
$C_{75}H_{87}N_6O_{18}Ga$
MW 1428.53 g.mol^{-1}

Gallium sulfate (28 mg, 0.07 mmol, 3.5 equiv) was solubilized in DMF (0.30 mL). A solution of NH_3 in 1,4-dioxane (0.5 M, 0.20 mL) was added to the mixture. A solution of dipeptide **SI-3** (10 mg, 0.02 mmol, 1.0 equiv) in DMF (0.30 mL) was added dropwise to the reaction mixture, which was stirred overnight at RT. The resulting crude product was precipitated into cold water, filtrated, and washed with water (3 × 1.0 mL). The solid was then solubilized in CH_2Cl_2, dried over Na_2SO_4, and filtrated, and the solvent was removed under reduced pressure to afford product **SI-5** as a white powder (29 mg, 0.02 mmol, 100% yield) mp 148−151 °C; IR ν_{max}: 3298, 2964, 2928, 1753, 1709, 1589, 1509, 1450, 1219, 1197, 1024, 758, 736 cm^{-1}; The broadness of the peaks in the ^1H NMR of product **SI-5** suggested that several conformers or several ligand arrangements around the Ga center might co-exist; therefore, the following chemical shifts are representative of the major *cis*-conformation of the ligand **SI-5**: ^1H NMR (400 MHz, CD_3CN, δ): 7.82 (m, 2H), 7.64 (m, 2H), 7.41 (m, 2H), 7.33 (m, 2H), 6.02 (d, J = 8.1 Hz, 1H), 4.87 (d, J = 17.9 Hz, 1H), 4.21 (m, 7H), 1.79 (m, 1H), 1.52 (m, 1H), 1.21 (m, 3H), 1.08 (m, 1H), 0.88 (m, 6H); $^{13}C\{^1H\}$ NMR (100 MHz, $CDCl_3$, δ): 170.3, 164.7, 156.3, 143.7, 143.6, 141.3 (2C), 127.8 (2C), 127.1 (2C), 125.1 (2C), 120.0 (2C), 67.2, 61.8, 54.0, 53.1, 47.2, 36.9, 24.7, 15.4, 13.9, 10.9; MALDI-TOF (m/z): $[M + Na]^+$ calcd for $C_{75}H_{87}N_6O_{18}GaNa$, 1451.5225; found, 1453. 2538.

■ ASSOCIATED CONTENT

Supporting Information

The Supporting Information is available free of charge at https://pubs.acs.org/doi/10.1021/acs.joc.0c01441.

https://dx.doi.org/10.1021/acs.joc.0c01441
J. Org. Chem. 2020, 85, 12329−12342

Tables of the selected results from the C- and N-terminal coupling optimization and epimerization are reported; complete experimental procedures and characterization data including ^{1}H, ^{13}C, NOESY, and HMBC NMR spectra, as well as HPLC chromatograms for measuring the levels of epimerization are available online (PDF)

CCDC 2009540 crystallographic data (for **12c**) (CIF)

AUTHOR INFORMATION

Corresponding Author

Stéphane P. Roche − *Department of Chemistry and Biochemistry and Center for Molecular Biology and Biotechnology, Florida Atlantic University, Boca Raton, Florida 33431, United States;* orcid.org/0000-0002-3019-2168; Email: sroche2@fau.edu

Author

Alexis D. Richaud − *Department of Chemistry and Biochemistry, Florida Atlantic University, Boca Raton, Florida 33431, United States*

Complete contact information is available at: https://pubs.acs.org/10.1021/acs.joc.0c01441

Author Contributions

S.P.R. and A.D.R. contributed equally to this work. This project was conceived by S.P.R. and the manuscript was written through the contributions of S.P.R. and A.D.R. All authors have given approval to the final version of the manuscript.

Notes

The authors declare no competing financial interest.

ACKNOWLEDGMENTS

We are very grateful for the financial support from the National Institutes of Health (NIGMS Grant: R21GM132754 to S.P.R and A.D.R.). The authors also thank Dr. Kari B. Basso at the Mass Spectrometry Research and Education Center from the Department of Chemistry at the University of Florida for the high-resolution mass spectrometry analysis supported by the NIH (S10 OD021758−01A1). The authors also thank Dr. Maren Pink, director of the Molecular Structure Center at the Indiana University Bloomington for the high-resolution crystal structure analysis (X-ray). We thank the NSF's ChemMatCARS Sector 15 supported by the Divisions of Chemistry (CHE) and Materials Research (DMR), National Science Foundation, under grant number NSF/CHE-1834750.

REFERENCES

(1) (a) Patch, J. A.; Barron, A. E. Mimicry of bioactive peptides via non-natural, sequence-specific peptidomimetic oligomers. *Curr. Opin. Chem. Biol.* **2002**, *6*, 872−877. (b) Yoo, B.; Kirshenbaum, K. Peptoid architectures: elaboration, actuation, and application. *Curr. Opin. Chem. Biol.* **2008**, *12*, 714−721. (c) Fowler, S. A.; Blackwell, H. E. Structure-function relationships in peptoids: Recent advances toward deciphering the structural requirements for biological function. *Org. Biomol. Chem.* **2009**, *7*, 1508−1524. (d) Sun, J.; Zuckermann, R. N. Peptoid Polymers: A Highly Designable Bioinspired Material. *ACS Nano* **2013**, *7*, 4715−4732.

(2) (a) Zuckermann, R. N.; Kerr, J. M.; Kent, S. B. H.; Moos, W. H. Efficient method for the preparation of peptoids [oligo(N-substituted glycines)] by submonomer solid-phase synthesis. *J. Am. Chem. Soc.* **1992**, *114*, 10646−10647. (b) Simon, R. J.; Kania, R. S.; Zuckermann, R. N.; Huebner, V. D.; Jewell, D. A.; Banville, S.; Ng, S.; Wang, L.; Rosenberg, S.; Marlowe, C. K. Peptoids: a modular approach to drug discovery. *Proc Natl. Acad. Sci. U.S.A.* **1992**, *89*, 9367−9371. (c) Zuckermann, R. N.; Kodadek, T. Peptoids as potential therapeutics. *Curr. Opin. Mol. Ther.* **2009**, *3*, 299−307.

(3) (a) Umezawa, K.; Nakazawa, K.; Ikeda, Y.; Naganawa, H.; Kondo, S. Polyoxypeptins A and B Produced by Streptomyces: Apoptosis-Inducing Cyclic Depsipeptides Containing the Novel Amino Acid (2S,3R)-3-Hydroxy-3-methylproline. *J. Org. Chem.* **1999**, *64*, 3034−3038. (b) Young, D. W.; Bender, A.; Hoyt, J.; McWhinnie, E.; Chirn, G.-W.; Tao, C. Y.; Tallarico, J. A.; Labow, M.; Jenkins, J. L.; Mitchison, T. J.; Feng, Y. Integrating high-content screening and ligand-target prediction to identify mechanism of action. *Nat. Chem. Biol.* **2008**, *4*, 59−68. (c) Oh, D.-C.; Poulsen, M.; Currie, C. R.; Clardy, J. Dentigerumycin: a bacterial mediator of an ant-fungus symbiosis. *Nat. Chem. Biol.* **2009**, *5*, 391−393. (d) Song, F.; He, H.; Ma, R.; Xiao, X.; Wei, Q.; Wang, Q.; Ji, Z.; Dai, H.; Zhang, L.; Capon, R. J. Structure revision of the Penicillium alkaloids haenamindole and citreoindole. *Tetrahedron Lett.* **2016**, *57*, 3851−3852. (e) Zhu, M.; Zhang, X.; Feng, H.; Dai, J.; Li, J.; Che, Q.; Gu, Q.; Zhu, T.; Li, D. Penicisulfuranols A−F, Alkaloids from the Mangrove Endophytic Fungus *Penicillium janthinellum* HDN13-309. *J. Nat. Prod.* **2017**, *80*, 71−75. (f) Dewapriya, P.; Prasad, P.; Damodar, R.; Salim, A. A.; Capon, R. J. Talarolide A, a Cyclic Heptapeptide Hydroxamate from an Australian Marine Tunicate-Associated Fungus, Talaromyces sp. (CMB-TU011). *Org. Lett.* **2017**, *19*, 2046−2049. (g) Shin, D.; Byun, W. S.; Moon, K.; Kwon, Y.; Bae, M.; Um, S.; Lee, S. K.; Oh, D.-C. Coculture of Marine Streptomyces sp. With Bacillus sp. Produces a New Piperazic Acid-Bearing Cyclic Peptide. *Front. Chem.* **2018**, *6*, 1−12.

(4) (a) Neilands, J. B. Hydroxamic Acids in Nature. *Science* **1967**, *156*, 1443−1447. (b) Emery, T. Biosynthesis and mechanism of action of hydroxamate-type siderochromes. *Microbial Iron Metabolism*; Elsevier, 1974; pp 107−123. (c) Palanché, T.; Blanc, S.; Hennard, C.; Abdallah, M. A.; Albrecht-Gary, A.-M. Bacterial Iron Transport: Coordination Properties of Azotobactin, the Highly Fluorescent Siderophore of *Azotobacter vinelandii*. *Inorg. Chem.* **2004**, *43*, 1137−1152. (d) Hermenau, R.; Ishida, K.; Gama, S.; Hoffmann, B.; Pfeifer-Leeg, M.; Plass, W.; Mohr, J. F.; Wichard, T.; Saluz, H.-P.; Hertweck, C. Gramibactin is a bacterial siderophore with a diazeniumdiolate ligand system. *Nat. Chem. Biol.* **2018**, *14*, 841−843.

(5) (a) Bianco, A.; Zabel, C.; Walden, P.; Jung, N. N-Hydroxy-Amide Analogues of MHC-Class I Peptide Ligands with Nanomolar Binding Affinities. *J. Pept. Sci.* **1998**, *4*, 471−478. (b) Hin, S.; Zabel, C.; Bianco, A.; Jung, G.; Walden, P. Cutting Edge: N-Hydroxy Peptides: A New Class of TCR Antagonists. *J. Immunol.* **1999**, *163*, 2363. (c) Bianco, A.; Kaiser, D.; Jung, G. N-Hydroxy Peptides as Substrates for α-Chymotrypsin. *J. Pept. Res.* **1999**, *54*, 544−548.

(6) (a) Bauer, L.; Exner, O. The Chemistry of Hydroxamic Acids and N-Hydroximides. *Angew. Chem., Int. Ed.* **1974**, *13*, 376−384. (b) Ye, Y.; Liu, M.; Kao, J. L. K.; Marshall, G. R. Peptide-Bond Modification for Metal Coordination: Peptides Containing Two Hydroxamate Groups. *Biopolymers* **2003**, *71*, 489−515. (c) Matsumoto, K.; Ozawa, T.; Jitsukawa, K.; Masuda, H. Synthesis, Solution Behavior, Thermal Stability, and Biological Activity of an Fe(III) Complex of an Artificial Siderophore with Intramolecular Hydrogen Bonding Networks. *Inorg. Chem.* **2004**, *43*, 8538−8546. (d) Geurink, P.; Klein, T.; Leeuwenburgh, M.; van der Marel, G.; Kauffman, H.; Bischoff, R.; Overkleeft, H. A peptide hydroxamate library for enrichment of metalloproteinases: towards an affinity-based metalloproteinase profiling protocol. *Org. Biomol. Chem.* **2008**, *6*, 1244−1250.

(7) (a) Ahmad, A. The Chemistry of α,N-Hydroxyamino Acids. *Bull. Chem. Soc. Jpn.* **1974**, *47*, 2583−2587. (b) Ottenheijm, H. C. J.; Herscheid, J. D. M. N-Hydroxy-α-amino Acids in Organic Chemistry. *Chem. Rev.* **1986**, *86*, 697−707. (c) Murahashi, S.-I.; Shiota, T. Short-step synthesis of amino acids and N-hydroxyamino acids from amines. *Tetrahedron Lett.* **1987**, *28*, 6469−6472. (d) Novak, M.; Bonham, G. A.; Mohler, L. K.; Peet, K. M. Acid-Catalyzed Hydrolysis of N-

Hydroxyacetanilides: Amide Hydrolysis versus Nitrogen-Oxygen Bond Heterolysis. *J. Org. Chem.* **1988**, *53*, 3903−3908.
(8) (a) Dupont, V.; Lecoq, A.; Mangeot, J. P.; Aubry, A.; Boussard, G.; Marraud, M. Conformational Perturbations Induced by N-Amination and N-Hydroxylation of Peptides. *J. Am. Chem. Soc.* **1993**, *115*, 8898−8906. (b) Takeuchi, Y.; Marshall, G. R. Conformational Analysis of Reverse-Turn Constraints by N-Methylation and N-Hydroxylation of Amide Bonds in Peptides and Non-Peptide Mimetics. *J. Am. Chem. Soc.* **1998**, *120*, 5363−5372.
(9) Crapster, J. A.; Stringer, J. R.; Guzei, I. A.; Blackwell, H. E. Design and Conformational Analysis of Peptoids Containing N-Hydroxy Amides Reveals a Unique Sheet-like Secondary Structure. *Biopolymers* **2011**, *96*, 604−616.
(10) (a) Busetti, V.; Ottenheijm, H. C. J.; Zeegers, H. J. M.; Ajò, D.; Casarin, M. Crystal and Molecular Structure of N-Acetyl N-Hydroxy α-Amino Acids. *Recl. Trav. Chim. Pays-Bas* **1987**, *106*, 151−156. (b) The Chemistry of Hydroxylamines, Oximes, and Hydroxamic Acids. In *Patai Series: The Chemistry of Functional Groups*; Rappoport, Z.; Liebman, J. F., Eds.; Wiley: Chichester, England; Hoboken, NJ, 2009; Vol. *1*.
(11) Jordan, P. A.; Paul, B.; Butterfoss, G. L.; Renfrew, P. D.; Bonneau, R.; Kirshenbaum, K. Oligo(N-Alkoxy Glycines): Trans Substantiating Peptoid Conformations. *Biopolymers* **2011**, *96*, 617−626.
(12) Richaud, A. D.; Roche, S. P. Structure-Property Relationship Study of N-(Hydroxy)Peptides for the Design of Self-Assembled Parallel β-Sheets. *ChemRxiv* **2020**, DOI: 10.26434/chemrxiv.12486236.v1.
(13) (a) Ahmad, A. Syntheses of α-Hydroxyamino Acids from α-Keto Acids. *Bull. Chem. Soc. Jpn.* **1974**, *47*, 1819−1820. (b) Kolasa, T.; Chimiak, A.; Kitowska, A. Esters of N-Benzyloxyamino Acids. *J. Prakt. Chem.* **1975**, *317*, 252−256. (c) Polonski, T.; Chimiak, A. Nitrones as Intermediates in the Synthesis of N-Hydroxyamino Acid Esters. *J. Org. Chem.* **1976**, *41*, 2092−2095.
(14) (a) Feenstra, R. W.; Stokkingreef, E. H. M.; Nivard, R. J. F.; Ottenheijm, H. C. J. An Efficient Synthesis of N-Hydroxy-α-Amino Acid Derivatives of High Optical Purity. *Tetrahedron Lett.* **1987**, *28*, 1215−1218. (b) Tokuyama, H.; Kuboyama, T.; Amano, A.; Yamashita, T.; Fukuyama, T. A Novel Transformation of Primary Amines to N-Monoalkylhydroxylamines. *Synthesis* **2000**, *2000*, 1299−1304. (c) Medina, S. I.; Wu, J.; Bode, J. W. Nitrone Protecting Groups for Enantiopure N-Hydroxyamino Acids: Synthesis of N-Terminal Peptide Hydroxylamines for Chemoselective Ligations. *Org. Biomol. Chem.* **2010**, *8*, 3405−3417.
(15) (a) Kolasa, T.; Chimiak, A. Unambiguous Synthesis of N-Hydroxypeptides. *Tetrahedron* **1977**, *33*, 3279−3284. (b) Maire, P.; Blandin, V.; Lopez, M.; Vallée, Y. Straightforward Synthesis of N -Hydroxy Peptides. *Synlett* **2003**, 671−674. (c) Hara, Y.; Akiyama, M. Peptide-Based Trihydroxamates as Models for Desferrioxamines. Iron(III)-Holding Properties of Linear and Cyclic N-Hydroxy Peptides with an l-Alanyl-l-Alanyl-N-Hydroxy-β-Alanyl Sequence. *Inorg. Chem.* **1996**, *35*, 5173−5180. (d) Lawrence, J.; Cointeaux, L.; Maire, P.; Vallée, Y.; Blandin, V. N-Hydroxy and N-Acyloxy Peptides: Synthesis and Chemical Modifications. *Org. Biomol. Chem.* **2006**, *4*, 3125−3141. (e) Ye, Y.; Liu, M.; Kao, J. L.-F.; Marshall, G. R. Novel Trihydroxamate-Containing Peptides: Design, Synthesis, and Metal Coordination. *Biopolymers* **2006**, *84*, 472−489. (f) Sarnowski, M. P.; Del Valle, J. R. N-Hydroxy peptides: solid-phase synthesis and β-sheet propensity. *Org. Biomol. Chem.* **2020**, *18*, 3690−3696. See also reference [5a].
(16) See Supporting Information for full experimental details.
(17) (a) Birnara, C.; Kessler, V. G.; Papaefstathiou, G. S. Mononuclear Gallium(III) Complexes Based on Salicylaldoximes: Synthesis, Structure and Spectroscopic Characterization. *Polyhedron* **2009**, *28*, 3291−3297. (b) Deshmukh, R. D. Preparation of Semiconductor Films. U.S. Patent WO2015/113733A1, 2015. See also ref 4c.
(18) (a) Valeur, E.; Bradley, M. Amide bond formation: beyond the myth of coupling reagents. *Chem. Soc. Rev.* **2009**, *38*, 606−631. (b) Dunetz, J. R.; Magano, J.; Weisenburger, G. A. Large-Scale Applications of Amide Coupling Reagents for the Synthesis of Pharmaceuticals. *Org. Process Res. Dev.* **2016**, *20*, 140−177.
(19) Asakura, T.; Okonogi, M.; Nakazawa, Y.; Yamauchi, K. Structural Analysis of Alanine Tripeptide with Antiparallel and Parallel β-Sheet Structures in Relation to the Analysis of Mixed β-Sheet Structures in *Samia cynthia* ricini Silk Protein Fiber Using Solid-State NMR Spectroscopy. *J. Am. Chem. Soc.* **2006**, *128*, 6231−6238.
(20) (a) Nowick, J. S.; Chung, D. M.; Maitra, K.; Maitra, S.; Stigers, K. D.; Sun, Y. An Unnatural Amino Acid that Mimics a Tripeptide β-Strand and Forms β-Sheetlike Hydrogen-Bonded Dimers. *J. Am. Chem. Soc.* **2000**, *122*, 7654−7661. (b) Phillips, S. T.; Rezac, M.; Abel, U.; Kossenjans, M.; Bartlett, P. A. "@-Tides": The 1,2-Dihydro-3(6H)-pyridinone Unit as a β-Strand Mimic. *J. Am. Chem. Soc.* **2002**, *124*, 58−66. (c) Laungani, A. C.; Slattery, J. M.; Krossing, I.; Breit, B. Supramolecular Bidentate Ligands by Metal-Directed in situ Formation of Antiparallel β-Sheet Structures and Application in Asymmetric Catalysis. *Chem. - Eur. J.* **2008**, *14*, 4488−4502. (d) Ong, Z. Y.; Gao, S. J.; Yang, Y. Y. Short Synthetic β-Sheet Forming Peptide Amphiphiles as Broad Spectrum Antimicrobials with Antibiofilm and Endotoxin Neutralizing Capabilities. *Adv. Funct. Mater.* **2013**, *23*, 3682−3692.
(21) For all peptide−peptoids studied, NMR data were recorded in a range of concentrations between 5 to 10 mM. The chemical shift deviations of amides and N-hydroxy amides were insignificant above 30 mM, which suggest that no aggregation occurs within the range of concentration studied.
(22) (a) Sui, Q.; Borchardt, D.; Rabenstein, D. L. Kinetics and Equilibria of Cis/Trans Isomerization of Backbone Amide Bonds in Peptoids. *J. Am. Chem. Soc.* **2007**, *129*, 12042−12048. (b) Laursen, J. S.; Engel-Andreasen, J.; Fristrup, P.; Harris, P.; Olsen, C. A. Cis−Trans Amide Bond Rotamers in β-Peptoids and Peptoids: Evaluation of Stereoelectronic Effects in Backbone and Side Chains. *J. Am. Chem. Soc.* **2013**, *135*, 2835−2844. (c) Stringer, J. R.; Crapster, J. A.; Guzei, I. A.; Blackwell, H. E. Construction of Peptoids with All Trans-Amide Backbones and Peptoid Reverse Turns via the Tactical Incorporation of N-Aryl Side Chains Capable of Hydrogen Bonding. *J. Org. Chem.* **2010**, *75*, 6068−6078.
(23) Wüthrich, K. *NMR of Proteins and Nucleic Acids*; Wiley: New York, 1986.
(24) (a) Abraham, M. H.; Abraham, R. J.; Byrne, J.; Griffiths, L. NMR Method for the Determination of Solute Hydrogen Bond Acidity. *J. Org. Chem.* **2006**, *71*, 3389−3394. (b) Abraham, M. H.; Abraham, R. J.; Acree, W. E.; Aliev, A. E.; Leo, A. J.; Whaley, W. L. An NMR Method for the Quantitative Assessment of Intramolecular Hydrogen Bonding; Application to Physicochemical, Environmental, and Biochemical Properties. *J. Org. Chem.* **2014**, *79*, 11075−11083.
(25) (a) Olivato, P. R.; Domingues, N. L. C.; Mondino, M. G.; Lima, F. S.; Zukerman-Schpector, J.; Rittner, R.; Colle, M. D. Stereochemical and electronic interaction studies of some N-methoxy-N-methyl-2-[(4′-substituted)phenylsulfinyl]propanamides. *J. Mol. Struct.* **2008**, *892*, 360−372. (b) Olivato, P. R.; Domingues, N. L. C.; Reis, A. K. C. A.; Vinhato, E.; Mondino, M. G.; Zukerman-Schpector, J.; Rittner, R.; Colle, M. D. Spectroscopic and theoretical studies of some N-methoxy-N-methyl-2-[(4′-substituted) phenylsulfonyl]propanamides. *J. Mol. Struct.* **2009**, *935*, 60−68.
(26) (a) Kaur, D.; Kohli, R. Hydrogen bond cooperativity in dimers of hydroxamic acids. *Int. J. Quantum Chem.* **2011**, *111*, 2931−2943. (b) Gupta, S. P. QSAR Studies on Hydroxamic Acids: A Fascinating Family of Chemicals with a Wide Spectrum of Activities. *Chem. Rev.* **2015**, *115*, 6427−6490.
(27) Shin, S. B. Y.; Kirshenbaum, K. Conformational Rearrangements by Water-Soluble Peptoid Foldamers. *Org. Lett.* **2007**, *9*, 5003−5006. see also reference 10.
(28) (a) Madison, V.; Schellman, J. Optical Activity of Polypeptides and Proteins. *Biopolymers* **1972**, *11*, 1041−1076. (b) Sreerama, N.; Woody, R. W. Computation and Analysis of Protein Circular Dichroism Spectra. *Methods Enzymol.*; Elsevier, 2004; Vol. *383*, pp 318−351. (c) Kung, V. M.; Cornilescu, G.; Gellman, S. H. Impact of

Strand Number on Parallel β-Sheet Stability. *Angew. Chem., Int. Ed.* **2015**, *54*, 14336−14339. (d) Guo, Y.; Wang, S.; Du, H.; Chen, X.; Fei, H. Silver Ion-Histidine Interplay Switches Peptide Hydrogel from Antiparallel to Parallel β-Assembly and Enables Controlled Antibacterial Activity. *Biomacromolecules* **2019**, *20*, 558−565.

(29) (a) Smith, A. M.; Williams, R. J.; Tang, C.; Coppo, P.; Collins, R. F.; Turner, M. L.; Saiani, A.; Ulijn, R. V. Fmoc-Diphenylalanine Self Assembles to a Hydrogel via a Novel Architecture Based on π−π Interlocked β-Sheets. *Adv. Mater.* **2008**, *20*, 37−41. (b) Ryan, D. M.; Doran, T. M.; Anderson, S. B.; Nilsson, B. L. Effect of C -Terminal Modification on the Self-Assembly and Hydrogelation of Fluorinated Fmoc-Phe Derivatives. *Langmuir* **2011**, *27*, 4029−4039. (c) Wang, Y.; Qi, W.; Wang, J.; Li, Q.; Yang, X.; Zhang, J.; Liu, X.; Huang, R.; Wang, M.; Su, R.; He, Z. Columnar Liquid Crystals Self-Assembled by Minimalistic Peptides for Chiral Sensing and Synthesis of Ordered Mesoporous Silica. *Chem. Mater.* **2018**, *30*, 7902−7911.

(30) (a) Stevens, E. S.; Sugawara, N.; Bonora, G. M.; Toniolo, C. Conformational Analysis of Linear Peptides. 3. Temperature Dependence of NH Chemical Shifts in Chloroform. *J. Am. Chem. Soc.* **1980**, *102*, 7048−7050. (b) Wang, C. K.; Northfield, S. E.; Colless, B.; Chaousis, S.; Hamernig, I.; Lohman, R.-J.; Nielsen, D. S.; Schroeder, C. I.; Liras, S.; Price, D. A.; Fairlie, D. P.; Craik, D. J. Rational Design and Synthesis of an Orally Bioavailable Peptide Guided by NMR Amide Temperature Coefficients. *Proc. Natl. Acad. Sci. U.S.A.* **2014**, *111*, 17504−17509. (c) Farley, K. A.; Che, Y.; Navarro-Vázquez, A.; Limberakis, C.; Anderson, D.; Yan, J.; Shapiro, M.; Shanmugasundaram, V.; Gil, R. R. Cyclic Peptide Design Guided by Residual Dipolar Couplings, J-Couplings, and Intramolecular Hydrogen Bond Analysis. *J. Org. Chem.* **2019**, *84*, 4803−4813.

(31) Seemingly, only one example of temperature dependence coefficients for N-(hydroxyl)peptides has been ″reported, see reference [5c]

(32) (a) Andersen, N. H.; Neidigh, J. W.; Harris, S. M.; Lee, G. M.; Liu, Z.; Tong, H. Extracting Information from the Temperature Gradients of Polypeptide NH Chemical Shifts. 1. The Importance of Conformational Averaging. *J. Am. Chem. Soc.* **1997**, *119*, 8547−8561. (b) Mahalakshmi, R.; Raghothama, S.; Balaram, P. NMR Analysis of Aromatic Interactions in Designed Peptide β-Hairpins. *J. Am. Chem. Soc.* **2006**, *128*, 1125−1138. (c) Körling, M.; Geyer, A. Beyond Natural Limitations: Long-Range Influence of Non-Natural Flexible and Rigid β-Turn Mimetics in a Native β-Hairpin Motif: Non-Natural β-Turn Mimetics in a Native β-Hairpin Motif. *Eur. J. Org. Chem.* **2015**, *2015*, 6448−6457. (d) Trainor, K.; Palumbo, J. A.; MacKenzie, D. W. S.; Meiering, E. M. Temperature Dependence of NMR Chemical Shifts: Tracking and Statistical Analysis. *Protein Sci.* **2020**, *29*, 306−314.

(33) (a) Kang, C. W.; Sarnowski, M. P.; Ranatunga, S.; Wojtas, L.; Metcalf, R. S.; Guida, W. C.; Del Valle, J. R. β-Strand mimics based on tetrahydropyridazinedione (tpd) peptide stitching. *Chem. Commun.* **2015**, *51*, 16259−16262. (b) Sarnowski, M. P.; Kang, C. W.; Elbatrawi, Y. M.; Wojtas, L.; Del Valle, J. R. Peptide N-Amination Supports β-Sheet Conformations. *Angew. Chem., Int. Ed.* **2017**, *56*, 2083−2086.

(34) (a) Langenhan, J. M.; Guzei, I. A.; Gellman, S. H. Parallel sheet secondary structure in β-peptides. *Angew. Chem., Int. Ed.* **2003**, *42*, 2402−2405. (b) Freire, F.; Fisk, J. D.; Peoples, A. J.; Ivancic, M.; Guzei, I. A.; Gellman, S. H. Diacid Linkers That Promote Parallel β-Sheet Secondary Structure in Water. *J. Am. Chem. Soc.* **2008**, *130*, 7839−7841. (c) Freire, F.; Gellman, S. H. Macrocyclic design strategies for small, stable parallel β-sheet scaffolds. *J. Am. Chem. Soc.* **2009**, *131*, 7970−7972. (d) Almeida, A. M.; Li, R.; Gellman, S. H. Parallel β-Sheet Secondary Structure Is Stabilized and Terminated by Interstrand Disulfide Cross-Linking. *J. Am. Chem. Soc.* **2012**, *134*, 75−78. (e) Calvelo, M.; Guerra, A.; Amorin, M.; Garcia-Fandino, R.; Lamas, A.; Granja, J. R. Parallel versus antiparallel β-sheet structure in cyclic peptide hybrids containing γ- or δ-cyclic amino acids. *Chem. - Eur. J.* **2020**, *26*, 5846−5858.

(35) Menges, F. "Spectragryph - optical spectroscopy software", Version 1.2.13, 2019, http://www.effemm2.de/spectragryph/ (accessed May 11, 2020).

(36) (a) Kruijtzer, J. A. W.; Hofmeyer, L. J. F.; Heerma, W.; Versluis, C.; Liskamp, R. M. J. Solid-Phase Syntheses of Peptoids Using Fmoc-Protected N-Substituted Glycines: The Synthesis of (Retro)Peptoids of Leu-Enkephalin and Substance P. *Chem. - Eur. J.* **1998**, *4*, 1570−1580. (b) Tijhuis, M. W.; Herscheid, J. D. M.; Ottenheijm, H. C. J. A Practical Synthesis of N-Hydroxy-α-Amino Acid Derivatives. *Synthesis* **2002**, *1980*, 890−893. (c) Wolfe, S.; Akuche, C.; Ro, S.; Wilson, M.-C.; Kim, C.-K.; Shi, Z. 5-Hydroxy[1,2]Oxazinan-3-Ones as Potential Carbapenem and D-Ala-D-Ala Surrogates. *Can. J. Chem.* **2003**, *81*, 915−936. (d) Nuti, E.; Orlandini, E.; Nencetti, S.; Rossello, A.; Innocenti, A.; Scozzafava, A.; Supuran, C. T. Carbonic Anhydrase and Matrix Metalloproteinase Inhibitors. Inhibition of Human Tumor-Associated Isozymes IX and Cytosolic Isozyme I and II with Sulfonylated Hydroxamates. *Bioorg. Med. Chem.* **2007**, *15*, 2298−2311. (e) Kaminker, R.; Anastasaki, A.; Gutekunst, W. R.; Luo, Y.; Lee, S.-H.; Hawker, C. J. Tuning of Protease Resistance in Oligopeptides through N-Alkylation. *Chem. Commun.* **2018**, *54*, 9631−9634.

https://dx.doi.org/10.1021/acs.joc.0c01441
J. Org. Chem. 2020, 85, 12329−12342